NASA TECHNICAL NOTE

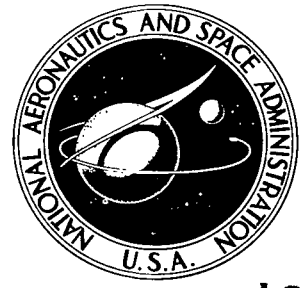

NASA TN D-8353 c.1

NASA TN D-8353

COMPARISON OF REMOTELY SENSED CONTINENTAL-SHELF WAVE SPECTRA WITH SPECTRA COMPUTED BY USING A WAVE REFRACTION COMPUTER MODEL

Lamont R. Poole

Langley Research Center
Hampton, Va. 23665

NATIONAL AERONAUTICS AND SPACE ADMINISTRATION • WASHINGTON, D. C. • DECEMBER 1976

1. Report No.	2. Government Accession No.	
NASA TN D-8353		

4. Title and Subtitle	5. Report Date
COMPARISON OF REMOTELY SENSED CONTINENTAL-SHELF WAVE SPECTRA WITH SPECTRA COMPUTED BY USING A WAVE REFRACTION COMPUTER MODEL	December 1976
	6. Performing Organization Code
7. Author(s)	8. Performing Organization Report No.
Lamont R. Poole	L-11072
	10. Work Unit No. 161-07-02-03
9. Performing Organization Name and Address NASA Langley Research Center Hampton, VA 23665	11. Contract or Grant No.
	13. Type of Report and Period Covered Technical Note
12. Sponsoring Agency Name and Address National Aeronautics and Space Administration Washington, DC 20546	14. Sponsoring Agency Code

15. Supplementary Notes

16. Abstract

An initial attempt was made to verify the Langley Research Center and Virginia Institute of Marine Science mid-Atlantic continental-shelf wave refraction model. The model was used to simulate refraction occurring during a continental-shelf remote sensing experiment conducted on August 17, 1973. Simulated wave spectra compared favorably, in a qualitative sense, with the experimental spectra. However, it was observed that most of the wave energy resided at frequencies higher than those for which refraction and shoaling effects were predicted. In addition, variations among the experimental spectra were so small that they were not considered statistically significant. In order to verify the refraction model, simulation must be performed in conjunction with a set of significantly varying spectra in which a considerable portion of the total energy resides at frequencies for which refraction and shoaling effects are likely.

17. Key Words (Suggested by Author(s))

Ocean wave refraction
Remote sensing
Wave refraction model

18. Distribution Statement

Unclassified - Unlimited

Subject Category 48

19. Security Classif. (of this report)	20. Security Classif. (of this page)	21. No. of Pages	22. Price*
Unclassified	Unclassified	43	$3.75

* For sale by the National Technical Information Service, Springfield, Virginia 22161

COMPARISON OF REMOTELY SENSED CONTINENTAL-SHELF WAVE SPECTRA WITH SPECTRA COMPUTED BY USING A WAVE REFRACTION COMPUTER MODEL

Lamont R. Poole
Langley Research Center

SUMMARY

An initial attempt to verify the Langley Research Center and Virginia Institute of Marine Science mid-Atlantic continental-shelf wave refraction model was made by using the model to simulate refraction occurring during a continental-shelf remote sensing experiment conducted on August 17, 1973. Simulated wave spectra compared favorably, in an overall qualitative sense, with experimental spectra. It was observed, however, that most of the wave energy resided at frequencies higher than those for which refraction and shoaling effects were predicted. In addition, variations among the experimental spectra were so small that they were considered statistically insignificant and, thus, not attributable to refraction and shoaling effects. In order to verify the refraction model, simulation must be performed in conjunction with a set of experimental spectra in which significant variation among the individual spectra is exhibited and in which a considerable portion of the total energy resides at frequencies for which refraction and shoaling effects are expected.

INTRODUCTION

Synoptic monitoring of ocean surface conditions from the NASA SEASAT-A satellite (ref. 1) promises to have a significant impact on future coastal-zone planning and management activities. Analytical models under development at the present time will use the broad-scale data from Seasat to provide short-term predictions of ocean surface conditions on a smaller spatial scale. These models could be of aid to the coastal-zone manager in areas such as disaster warning, pollution dispersal, or site selection for offshore and coastal facilities.

The wave refraction model is one analytical procedure which could play an integral role in an effective coastal-zone management program. Given reference wave measurements at points along the outer edge of the continental shelf, the refraction model would predict the behavior of the waves as they cross the shelf and impinge on the shoreline. Of course, before a wave refraction model can be used in an operational management or planning program, its computations must be verified by comparison with actual continental-shelf wave measurements for a wide range of wave conditions.

The present paper describes a procedure used in an initial attempt to verify the Langley Research Center (LaRC) and Virginia Institute of Marine Science (VIMS) wave refraction model described in reference 2. Experimental wave measurements were obtained by using an airborne laser profilometer (ref. 3) which was flown over an approximately 60-nautical-mile stretch of the continental shelf off Assateague Island, Maryland, on August 17, 1973. Energy density spectra derived from the experimental measurements are compared with simulated spectra computed by using the LaRC-VIMS refraction model according to the procedure of Chao (ref. 4). Discussion of agreement between computed and experimental spectra leads to recommendations for future attempts at model verification.

SYMBOLS

b	ray separation distance, meters
d	water depth, meters
E	energy density between ray pair j and $j + 1$, joules/meter^2
$F(f)$	normalized energy amplification function
f	wave frequency, hertz
$H_{1/3}$	significant wave height, average height of highest one-third of waves, meters
j	wave ray index
K_r	refraction coefficient, defined by equation (2)
K_s	shoaling coefficient, defined by equation (3)
k	wave number, meters^{-1}
$S(f)$	spectral density, meters^2/hertz
T	wave period, seconds
x,y	distances along axes of wave refraction model, nautical miles
α	angle from which waves are propagating, as defined in figure 4, degrees

Subscript:

o	initial (deep-water) value

A bar over a symbol indicates spatial average over a flight-track segment.

WAVE MEASUREMENT EXPERIMENT

The nominal plan chosen for airborne continental-shelf wave measurement experiments consists of two phases. During the first phase the aircraft flies offshore for a distance of approximately 60 nautical miles in a direction opposite to that of the local (onshore) wind and at an altitude of 1.6 kilometers. Along this flight track, reference photographs are taken of the ocean surface with an aerial mapping camera. The second phase consists of a return (onshore) flight in the direction of the local wind and at an altitude of 160 meters. During this phase a continuous profile of the ocean surface along the flight track is obtained by using a laser profilometer in the mode described in reference 3.

The present wave measurement experiment was conducted on August 17, 1973, aboard a NASA C-54 aircraft stationed at Wallops Flight Center, Virginia. Weather conditions in effect during and for several hours in advance of the flight included scattered clouds at an altitude of 650 meters and a visibility of 6 to 7 nautical miles. Winds were from the northeast, shifting to the east-northeast at speeds of 5 to 8 meters/second. On the basis of these wind data, the nominal bearing for the offshore flight track was selected as 070° from true north. A navigational buoy located off Assateague Island, Maryland, near longitude 75° W and latitude 38° N was chosen arbitrarily as a geographical reference point over which to fly and initiate the experiment.

The offshore phase of the experiment was begun at 17:46 GMT on August 17. Onboard navigation was provided by a LORAN navigation system with which readings were made at 10-nautical-mile intervals to allow for course corrections as necessary. Onboard LORAN readings taken at points from 0 to 60 nautical miles offshore from the reference buoy were mapped onto a Mercator projection by using a U.S. Naval Oceanographic Office LORAN navigational chart. Shown in figure 1 is the offshore flight track faired through the actual data points. Some deviation from the nominal 070° bearing is evident in figure 1. For the purposes of this paper, the possibility of errors in the LORAN readings is disregarded and the faired flight track is considered exact. Reference photographs were taken during this offshore flight with the aerial mapping camera equipped with a yellow filter and 9-inch format film. Three of the reference photographs are presented in figure 2, with parts (a), (b), and (c) first (shoreward), middle, and last portions of the flight track, respectively. In each figure, the aircraft was flying in a direction from left to right (offshore), and the majority of waves are traveling in nearly the same direction.

The offshore phase of the experiment was concluded at 18:06 GMT at a point approximately 60 nautical miles from the reference buoy. The aircraft was then brought down to the 160-meter altitude for the return flight, which was begun at 18:15 GMT at a nominal bearing of 250° from true north and a nominal speed of 80 meters/second. Onboard LORAN readings taken at 10-nautical-mile intervals on the return flight were again mapped onto a Mercator projection. The actual onshore flight track faired through the projected LORAN data points is shown in figure 3. Considerable deviation from the nominal bearing is evident, but, again, the faired flight track is considered

exact. During this phase of the experiment, a continuous profile of the ocean surface (with a maximum resolution of 10 cm) was obtained by using the laser profilometer. The laser data were recorded in analog form on magnetic tape between the times of 18:15:30 GMT and 18:35:30 GMT.

LASER DATA ANALYSIS

In order to provide quasi-homogeneous data sets for the subsequent spectral analysis, the magnetic tape record of laser profilometer data was partitioned into 10 adjacent but independent sections of 2-minute length each. Each section was digitized using an interval of 0.04 second and then treated by a high-pass digital filter (ref. 5) in order to remove extraneous energy at very low true frequencies (less than 0.06 Hz) attributed to vertical aircraft motions. On the basis of evidence from a similar wave measurement experiment (ref. 6), aircraft pitch and roll motions were assumed to have little influence on the data record obtained. Raw apparent spectra (spectra observed from the moving aircraft reference frame) for each filtered section were obtained by computing the Fourier cosine transform of the autocorrelation function (to 150 lags) of the filtered section in question, according to the method of Blackman and Tukey (ref. 7). Such a treatment of data obtained over a finite spatial increment produces, in essence, a spectrum which is a spatial average of local spectra over the increment in question (ref. 8). The raw apparent spectra were then treated by the Hamming weighted averaging process (ref. 9, pp. 447-448) to obtain smoothed apparent spectra with 80 percent confidence that repeated measurements of the same wave field would result in spectral density values lying between 0.71 and 1.31 times the values computed from the initial measurements.

For the purposes of the present paper, it was assumed that directional spreading in the wave field and deviations of the aircraft flight track from the mean direction of wave propagation could be neglected. Therefore, the smoothed apparent spectra were transformed into true spectra in a stationary reference frame by using the unidirectional transformation technique presented in reference 10. In order to obtain spatially averaged depth values along the various flight-track segments, which were required for the transformation, the onshore flight track was mapped into the rectangular coordinate system of the LaRC-VIMS wave refraction model (fig. 4). The flight track was divided by tick marks into 2-minute segments, which are numbered from 1 to 10 (advancing shoreward), corresponding to the previously computed apparent spectra. Segment 1 was found to lie outside the seaward boundary of the refraction model coordinate system and was selected to provide the reference spectrum to be used in subsequent calculations. The average depth $\bar{d}$ along segment 1 was estimated from an auxiliary bathymetry chart to be 100 meters, and the resulting transformed spectrum, designated as the reference deep-water spectrum, is shown in figure 5.

A portion of segment 2 was also found to lie outside the seaward boundary of the model coordinate system. Since there would be no capability for simulating in full the propagation and refraction of the reference spectrum through segment 2, the apparent spectrum for this segment was discarded. Average depth values along segments 3 to 10 were computed by averaging depth

values at points along appropriate rays in the wave refraction diagrams which were constructed for use in simulating refraction of the reference deep-water spectrum (to be discussed in the following section). The resulting transformed spectra for segments 3 to 10 are shown in figure 6.

SIMULATION OF SPECTRUM REFRACTION

Because of the weak local winds in effect during the onshore flight experiment, it was assumed that any changes observed in the spectra obtained over the flight track were due to refraction and shoaling effects rather than to local wave generation. Simulation of these refraction and shoaling effects was performed by using the LaRC-VIMS monochromatic wave refraction model according to a procedure such as the one outlined by Pierson, Neumann, and James (ref. 11) and implemented by Chao (ref. 4). It was assumed that the deep-water spectrum could be represented, with wave-wave interaction neglected, by a linear superposition of monochromatic waves traveling initially in a single direction. (This assumption correlates with the neglect of directional spreading in analysis of the laser data.) The first step in the simulation procedure was then to construct a refraction diagram for each monochromatic wave used to approximate the spectrum.

The LaRC-VIMS refraction program was altered for convenience in construction of the required refraction diagrams. Computations were limited to a family of wave rays (orthogonals to wave crests), each separated by 1 nautical mile in deep water, in the vicinity of the onshore flight track. Instructions were added to the program to initiate ray computations at deep-water points lying along a crest line orthogonal to the initial ray direction in order to reference all computations to an intial time. Succeeding computations were then performed in fixed time increments, and tick marks were added to rays in the constructed refraction diagram at spatial intervals corresponding to 5 time steps. The initial angle α_o selected for all waves in the approximating series was the mean acute angle between the onshore flight track and the X-axis of the model coordinate system, which was computed to be 67^o. Refraction diagrams were then computed for waves propagating from this direction and ranging in period from $T = 6$ seconds to $T = 14$ seconds. This period range corresponds to a frequency range from $f = 0.1667$ hertz to $f = 0.0714$ hertz. Little energy was observed in the transformed experimental spectra (figs. 5 and 6) at frequencies lower than 0.0714 hertz, and waves at frequencies higher than 0.1667 hertz were found to undergo little or no refraction. Sample refraction diagrams are presented in figure 7 for periods $T = 6$, 8, 10, 12, and 14 seconds. The circular symbols in each figure denote LORAN aircraft position data for the onshore flight track.

Energy Amplification Functions

Variations in wave energy due to refraction and shoaling effects can be estimated according to linear theory by considering the wave energy between two vertical planes which are orthogonal to the wave crests and intersect with the surface to produce wave rays. If reflection, percolation, and bot-

tom friction are neglected and it is assumed that no energy is transmitted across wave rays, then for a wave of frequency f_n, the energy density E at some point shoreward from a reference deep-water location and bounded by ray pair j and $j + 1$ can be written as

$$E(f_n) = E_o(f_n)\, K_r^2(f_n)\, K_s^2(f_n) \tag{1}$$

where E_o is the initial (deep-water) energy density between ray pair j and $j + 1$; K_r is the local refraction coefficient, defined by

$$K_r = \left(\frac{b_o}{b}\right)^{1/2} \tag{2}$$

where b_o is the initial (deep-water) distance between rays j and $j + 1$ (fixed as 1 n. mi.) and b is the distance between rays j and $j + 1$ at the local point of interest; and K_s is the local shoaling coefficient, defined by (ref. 2, p. 8)

$$K_s = \left(\frac{2 \cosh^2 kd}{2kd + \sinh 2kd}\right)^{1/2} \tag{3}$$

where d is the depth at the point of interest. By computing the energy density ratios E/E_o at the point of interest for waves of varying frequency, a normalized energy amplification function $F(f)$ can be constructed as a function of wave frequency. Then, with a reference deep-water spectral density $S_o(f)$ given, the local unidirectional refracted spectral density $S(f)$ can be computed as the product of the reference spectral density and the normalized energy amplification function, or,

$$S(f) = S_o(f)\, F(f) \tag{4}$$

However, the wave spectra computed from the experimental laser profiles represent spatial averages of local spectra over the various flight-track segments, as discussed previously. Accordingly, spatially averaged amplification functions $\overline{F(f)}$ were computed for use in the simulation procedure by first superimposing the aircraft flight track onto each of the constructed refraction diagrams as shown, for example, in figure 8 for a wave period $T = 10$ seconds. A spatially averaged normalized energy ratio $\overline{E/E_o}$ for segment 8, for example, was computed by averaging local energy ratios computed by the refraction program at points between p_1 and p_2. Performance of such computations for each monochromatic wave used to approximate the spectrum (T ranging from 6 to 14 sec) resulted in construction of average energy amplification functions for each segment, in the frequency range from 0.0714 hertz to 0.1667 hertz. For frequencies less than 0.0714 hertz, the respective amplification functions were assumed to be equal to their values at

0.0714 hertz, while for frequencies greater than 0.1667 hertz, the amplification functions were assumed to be 1.0. Plots of the amplification functions for the eight flight-track segments are given in figure 9, in which the dashed portions of the plots indicate assumed values.

Simulated Refracted Spectra

Simulated refracted spectra for flight-track segments 3 to 10 were computed by multiplying, according to equation (4), the reference deep-water spectrum (fig. 5) by the spatially averaged energy amplification function $\overline{F(f)}$ for each of the segments. The resultant simulated spectra are compared with the experimentally determined spectra in figure 10.

DISCUSSION

In an overall qualitative manner the simulated spectra for all eight flight-track segments compare favorably with the respective experimental spectra. With respect to verification of the refraction model, however, the results are less favorable. It can be seen that nearly all the energy in the various spectra resides at frequencies greater than 0.12 hertz. Since the computed amplification functions were essentially 1.0 in this frequency range for all flight-track segments, the simulated spectra are identically equal to the reference deep-water spectrum in this range. In addition, if the spectra in figure 10 are compared with the reference deep-water spectrum (fig. 5), the spectra for each flight-track segment appear to lie, for the most part, within the 80-percent confidence limits of the reference spectrum. Thus, in an overall manner the changes in the various spectra relative to the reference deep-water spectrum are statistically insignificant at the 80-percent confidence level.

Since the various spectra exhibit a similar characteristic shape, differences among the spectra can be discussed from a more quantitative approach by considering the significant height $H_{1/3}$, which, under the assumption of a Gaussian distribution of wave heights, is equal to 4 times the square root of the area under the spectrum (ref. 12, pp. 22). The areas under simulated and experimental spectra for flight-track segments 3 to 10 were computed by trapezoidal integration, and the resultant significant heights were compared with the significant height for the reference deep-water spectrum. Relative changes of 0 to 2 percent in the simulated significant heights substantiate the observation that most of the energy in the reference spectrum resided at frequencies above those for which refraction effects were predicted. A maximum relative change of 9 percent was found in the experimental significant heights. Such a change would correspond to a 19-percent maximum difference in spectral density levels, which falls within approximately $\pm$30-percent band limits that must be exceeded to attain a statistically significant difference.

The foregoing discussion indicates that in order to verify the LaRC-VIMS refraction model, experimental data must be obtained under conditions such that a considerable portion of the total wave energy resides at frequencies

lower than those experienced in the present analysis. In addition, there must be variations among the individual wave spectra to a degree that the variations can be attributed with statistical significance to physical causes, namely shoaling and refraction, rather than to random fluctuations. To achieve statistical significance while retaining reasonable frequency resolution, future analyses might require much longer data record lengths or digitization using a much smaller interval.

CONCLUDING REMARKS

The present paper has described the procedure used in an initial attempt to verify the Langley Research Center and Virginia Institute of Marine Science mid-Atlantic continental-shelf wave refraction model. Experimental spectra were obtained along a 60-nautical-mile track in the region off Assateague Island, Maryland, on August 17, 1973, by using a laser profilometer mounted aboard a NASA C-54 aircraft. The refraction model was then used in a linear superposition mode to simulate the spectrum refraction occurring during the flight experiment.

The simulated spectra compared favorably with the experimental spectra in an overall qualitative sense. It was observed, however, that most of the wave energy resided at frequencies higher than those for which refraction effects were predicted. In addition, variations among the experimental spectra were statistically insignificant and thus could not be attributed to physical causes, namely shoaling and refraction. In order to verify the refraction model, simulation must be performed in conjunction with a set of experimental spectra in which significant variation among the individual spectra is exhibited and in which a considerable portion of the total wave energy occurs at lower frequencies than experienced in the present analysis.

Langley Research Center
National Aeronautics and Space Administration
Hampton, VA 23665
November 22, 1976

REFERENCES

1. McCandless, S. Walter, Jr.: SEASAT-A - A User Oriented Systems Design. Proceedings of the International Symposium on Applications of Marine Geodesy, Mar. Technol. Soc., c.1974, pp. 67-74.

2. Goldsmith, Victor; Morris, W. Douglas; Byrne, Robert J.; and Whitlock, Charles H.: Wave Climate Model of the Mid-Atlantic Shelf and Shoreline (Virginian Sea) - Model Development, Shelf Geomorphology, and Preliminary Results. NASA SP-358, VIMS SRAMSOE No. 38, 1974.

3. Schule, John J., Jr.; Simpson, Lloyd S.; and DeLeonibus, P. S.: A Study of Fetch-Limited Wave Spectra With an Airborne Laser. J. Geophys. Res., vol. 76, no. 18, June 20, 1971, pp. 4160-4171.

4. Chao, Yung-Yao: Wave Refraction Phenomena Over the Continental Shelf Near the Cheasapeake Bay Entrance. Tech. Mem. No. 47, Coastal Eng. Res. Center, U.S. Army Corps Eng., Oct. 1974.

5. Linnette, H. M.: Statistical Filters for Smoothing and Filtering Equally Spaced Data. Res. Rep. 1049, U.S. Navy Electron. Lab., July 10, 1961.

6. Barnett, T. P.; and Wilkerson, J. C.: On the Generation of Ocean Wind Waves as Inferred From Airborne Radar Measurements of Fetch-Limited Spectra. J. Mar. Res., vol. 25, no. 3, Sept. 15, 1967, pp. 292-328.

7. Blackman, R. B.; and Tukey, J. W.: The Measurement of Power Spectra From the Point of View of Communications Engineering. Dover Publ., Inc., c.1958.

8. Tayfun, M. A.; Yang, C. Y.; and Hsiao, G. C.: Optimal Design for Wave Spectrum Estimates. J. Geophys. Res., vol. 80, no. 15, May 20, 1975, pp. 1937-1947.

9. Kinsman, Blair: Wind Waves - Their Generation and Propagation on the Ocean Surface. Prentice-Hall, Inc., c.1965.

10. Poole, Lamont R.: Transformation of Apparent Ocean Wave Spectra Observed From an Aircraft Sensor Platform. NASA TN D-8246, 1976.

11. Pierson, Willard J., Jr.; Neumann, Gerhard; and James, Richard W.: Practical Methods for Observing and Forecasting Ocean Waves by Means of Wave Spectra and Statistics. H. O. Publ. No. 603, U.S. Naval Oceanogr. Office, 1971.

12. Neumann, Gerhard; and Pierson, Willard J., Jr.: Known and Unknown Properties of the Frequency Spectrum of a Wind-Generated Sea. Ocean Wave Spectra, Prentice-Hall, Inc., c.1963, pp. 9-25.

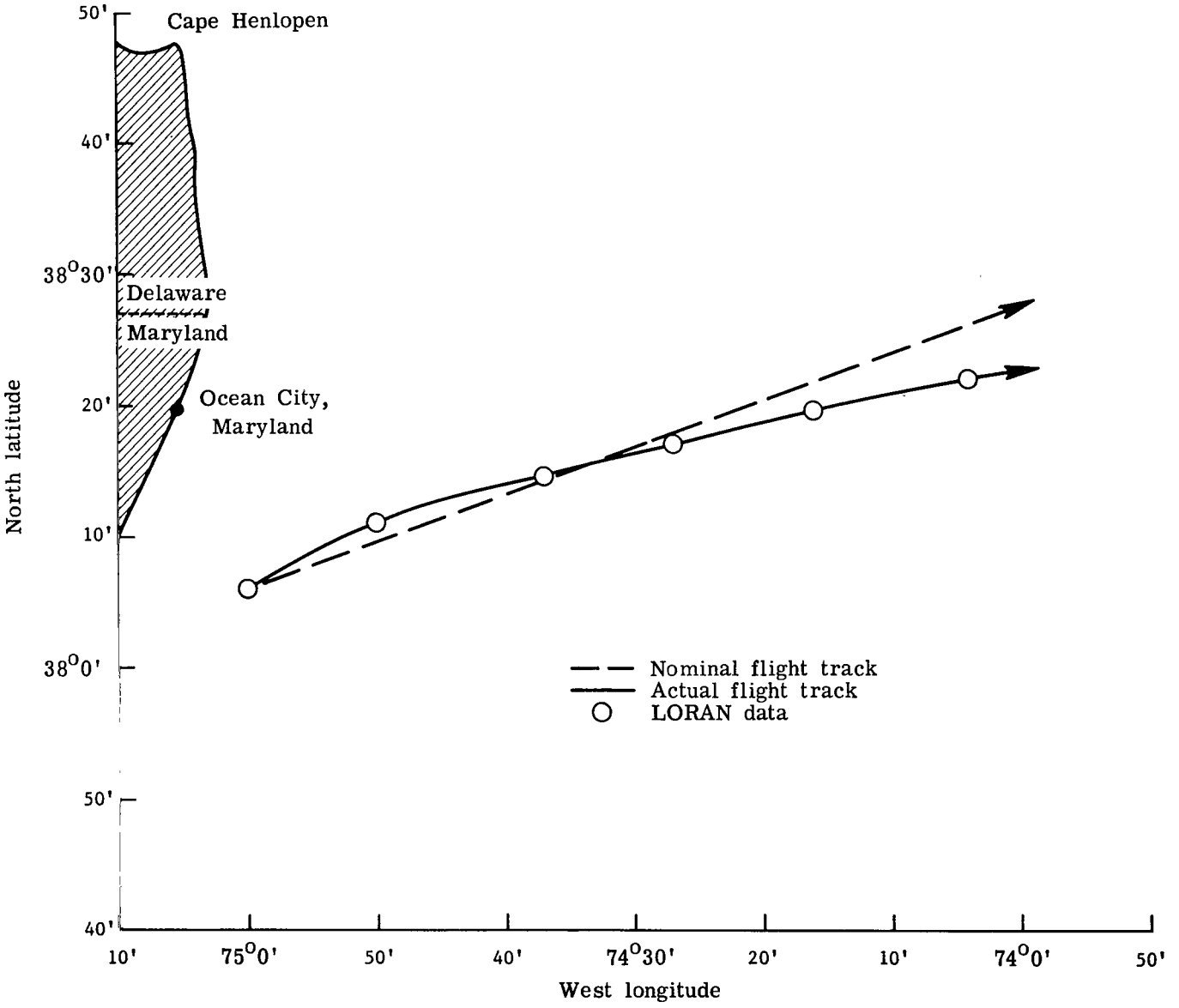

Figure 1.- Offshore flight track for wave measurement experiment.

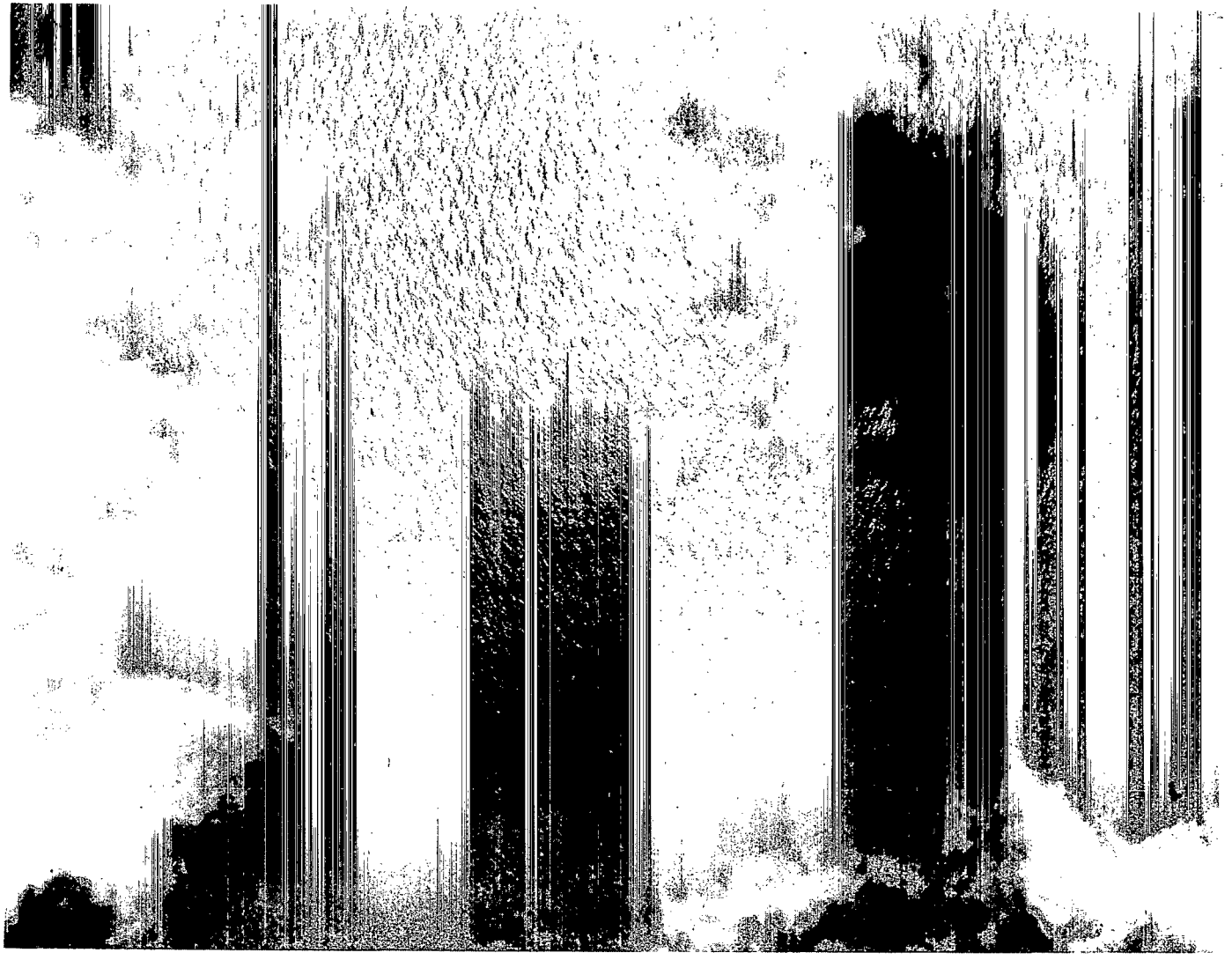

L-76-7502

(a) Shoreward portion of flight track.

Figure 2.- Reference photographs of wave field taken during offshore phase of wave measurement experiment.

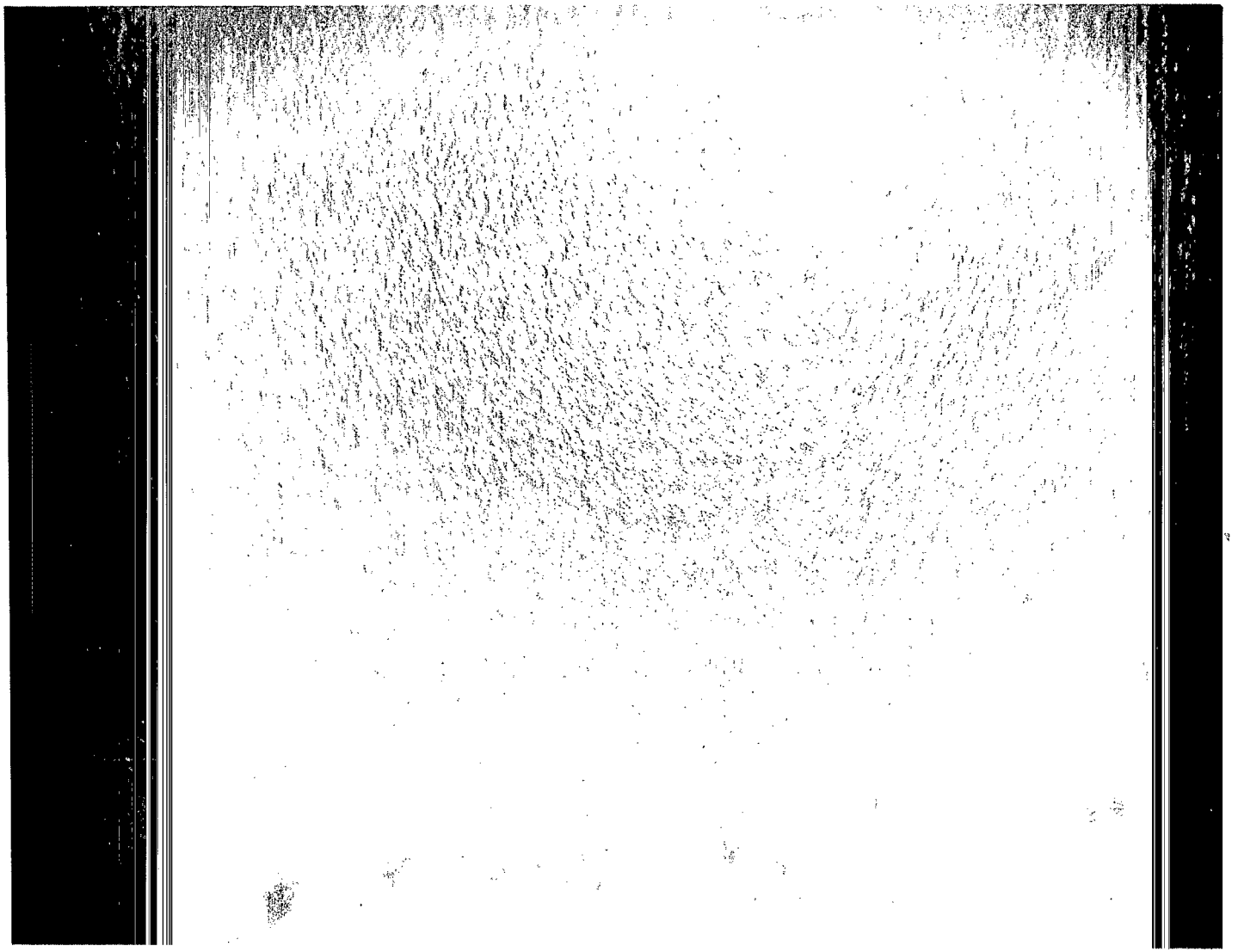

L-76-7503

(b) Middle portion of flight track.

Figure 2.- Continued.

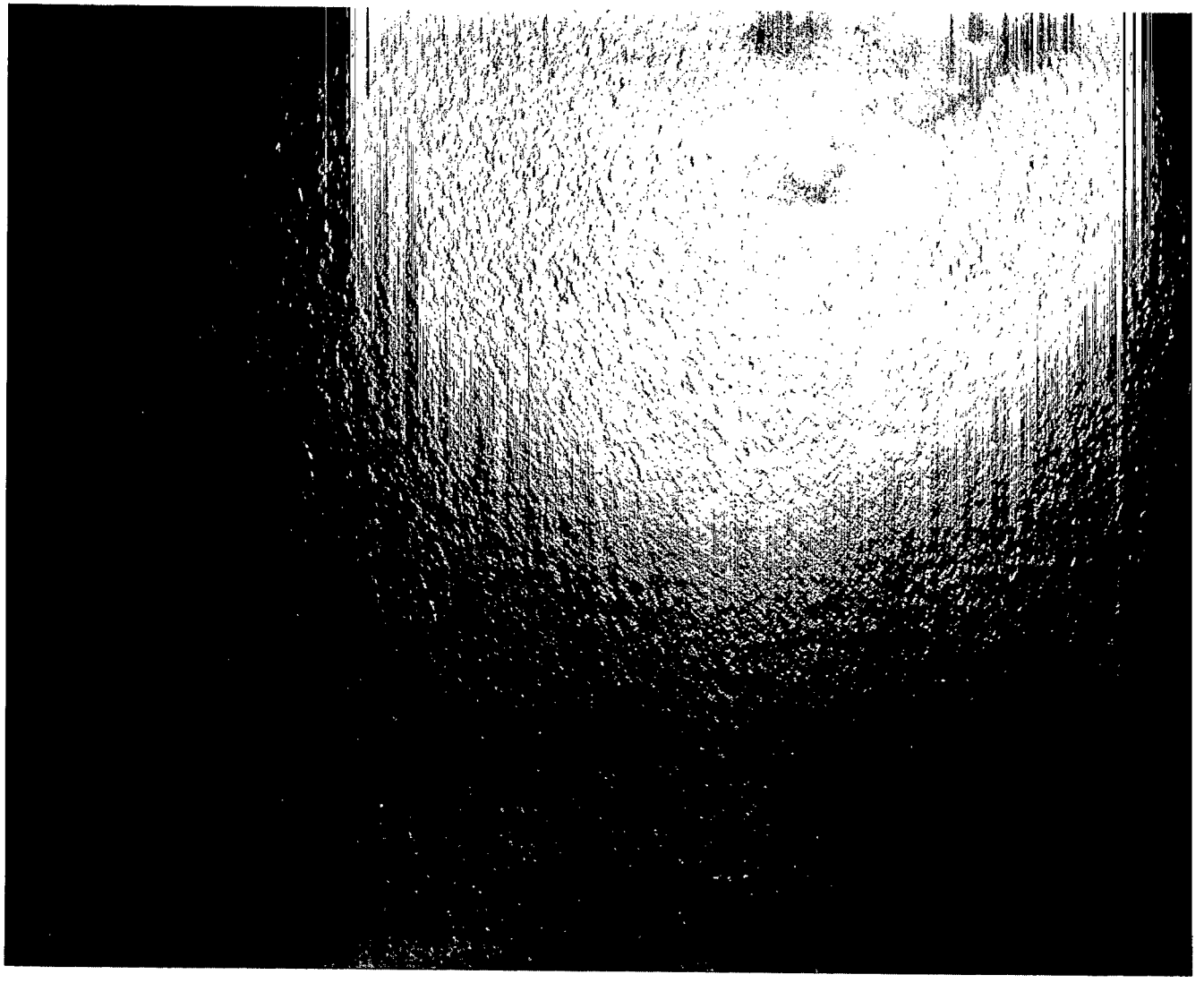

L-76-7504

(c) Final (seaward) portion of flight track.

Figure 2.- Concluded.

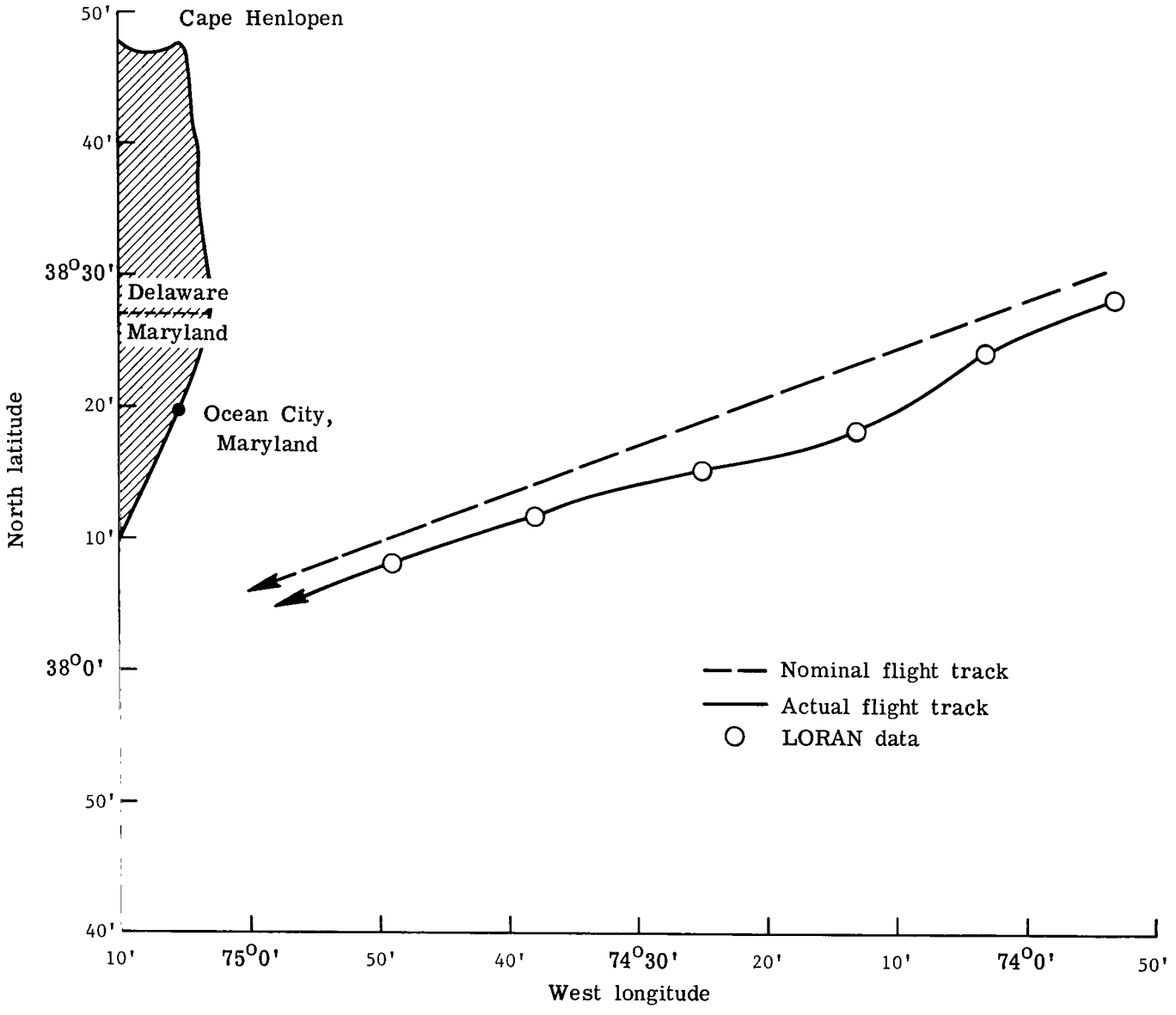

Figure 3.- Onshore flight track for wave measurement experiment.

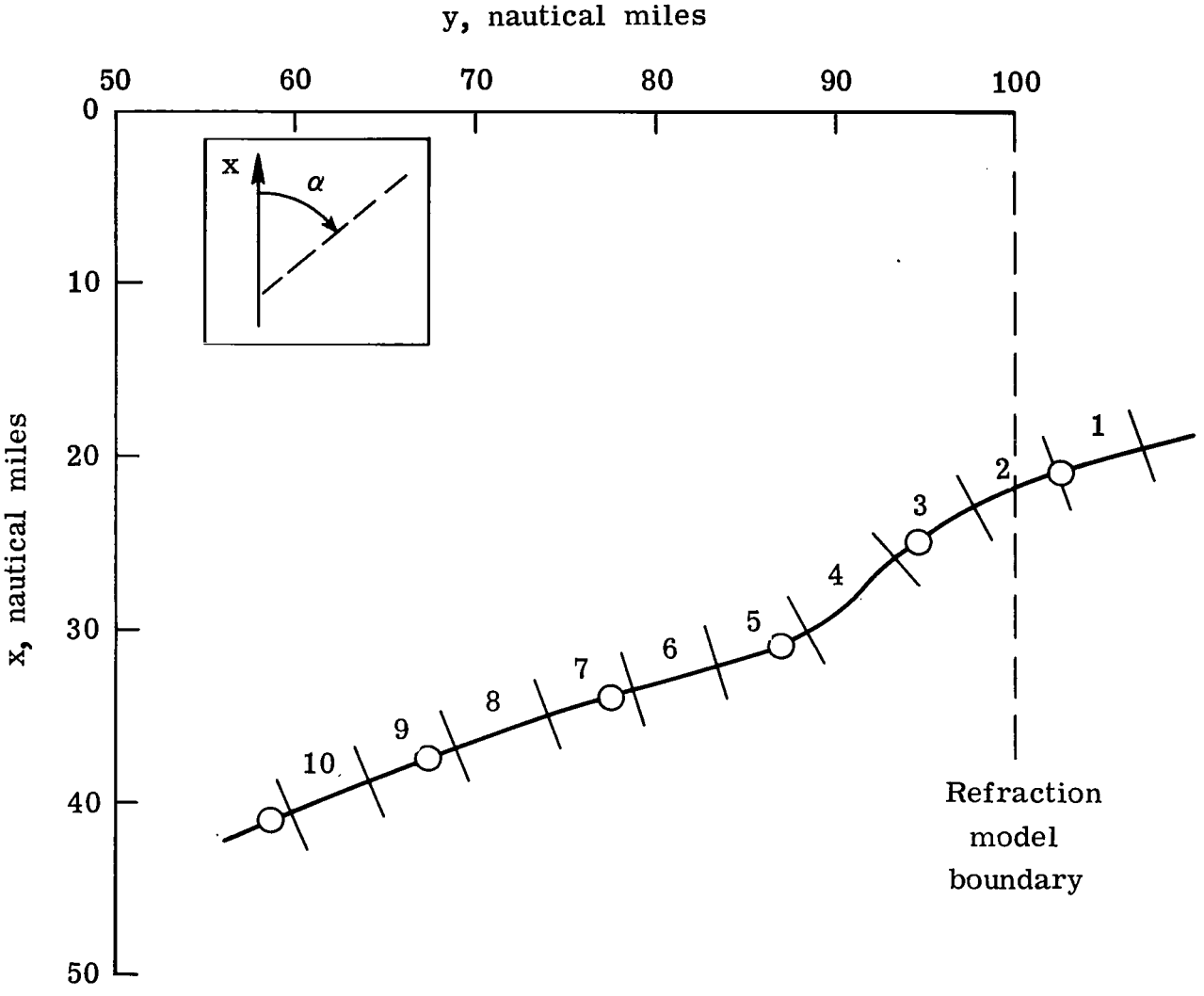

Figure 4.- Onshore flight track in refraction model coordinate system divided into numbered 2-minute segments. Circular symbols denote LORAN data.

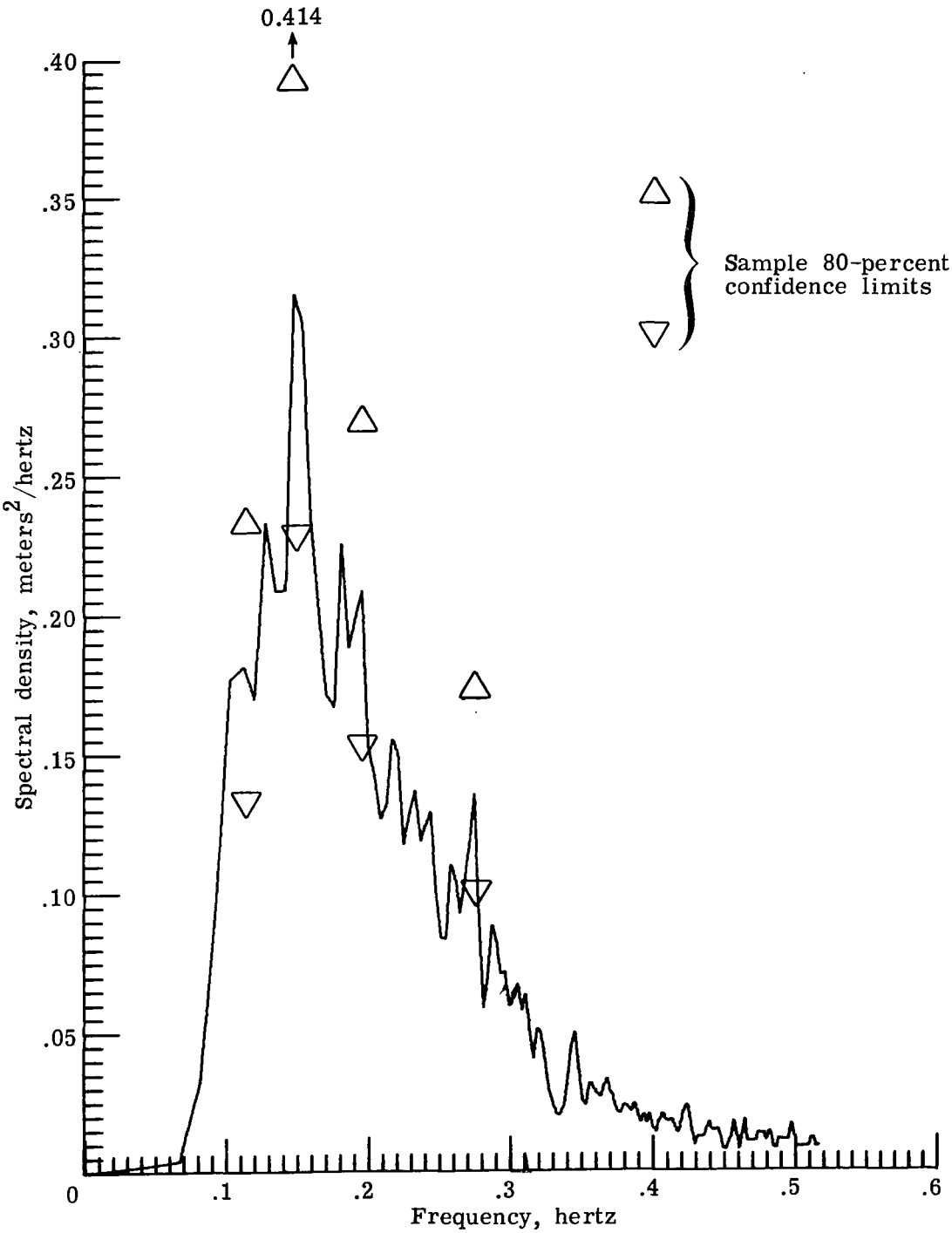

Figure 5.- Reference deep-water wave spectrum, transformed for $\bar{d}$ = 100 meters.

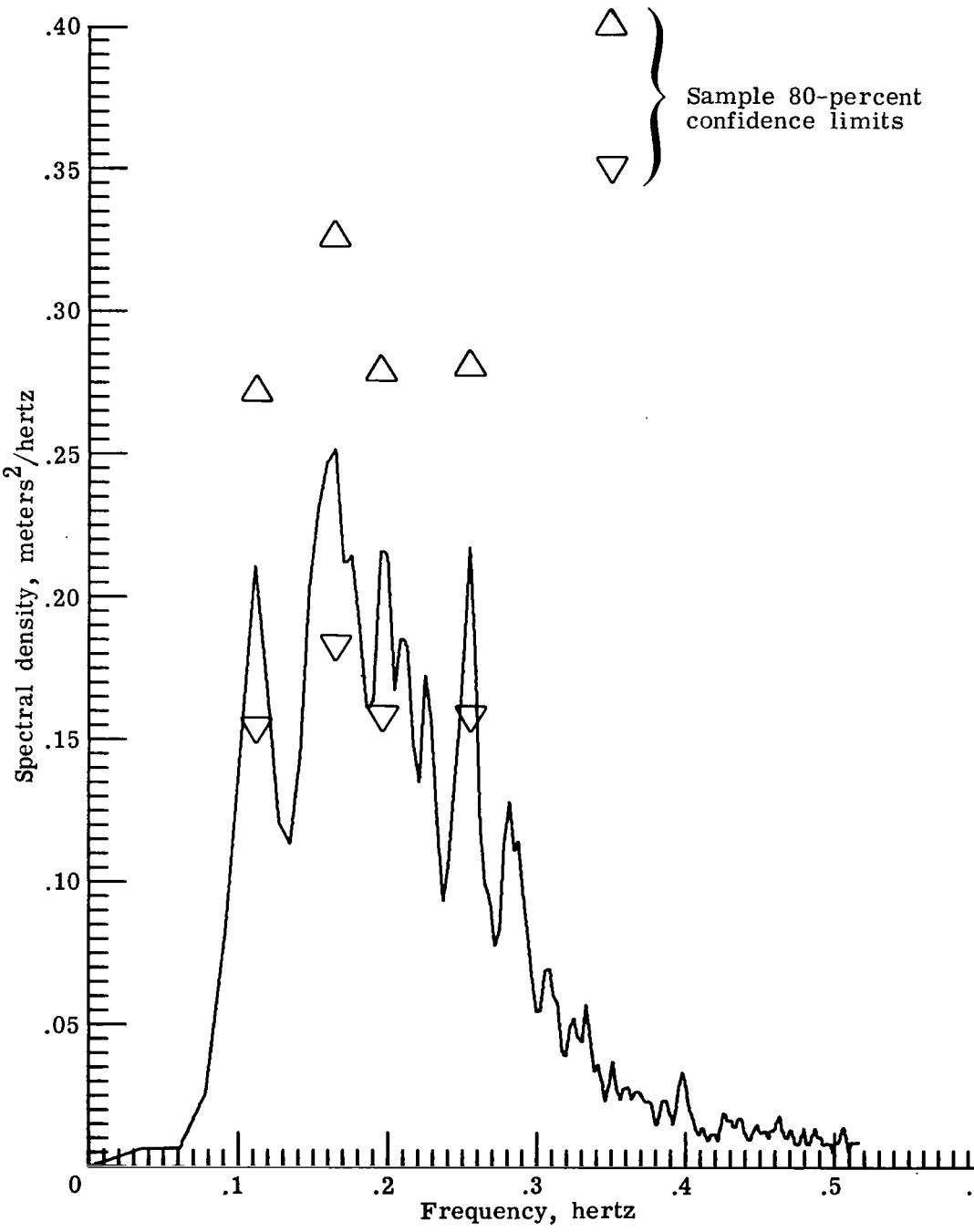

(a) Segment 3; $\bar{d}$ = 58 meters.

Figure 6.- Wave spectra for flight-track segments, transformed for $\bar{d}$ of respective segments.

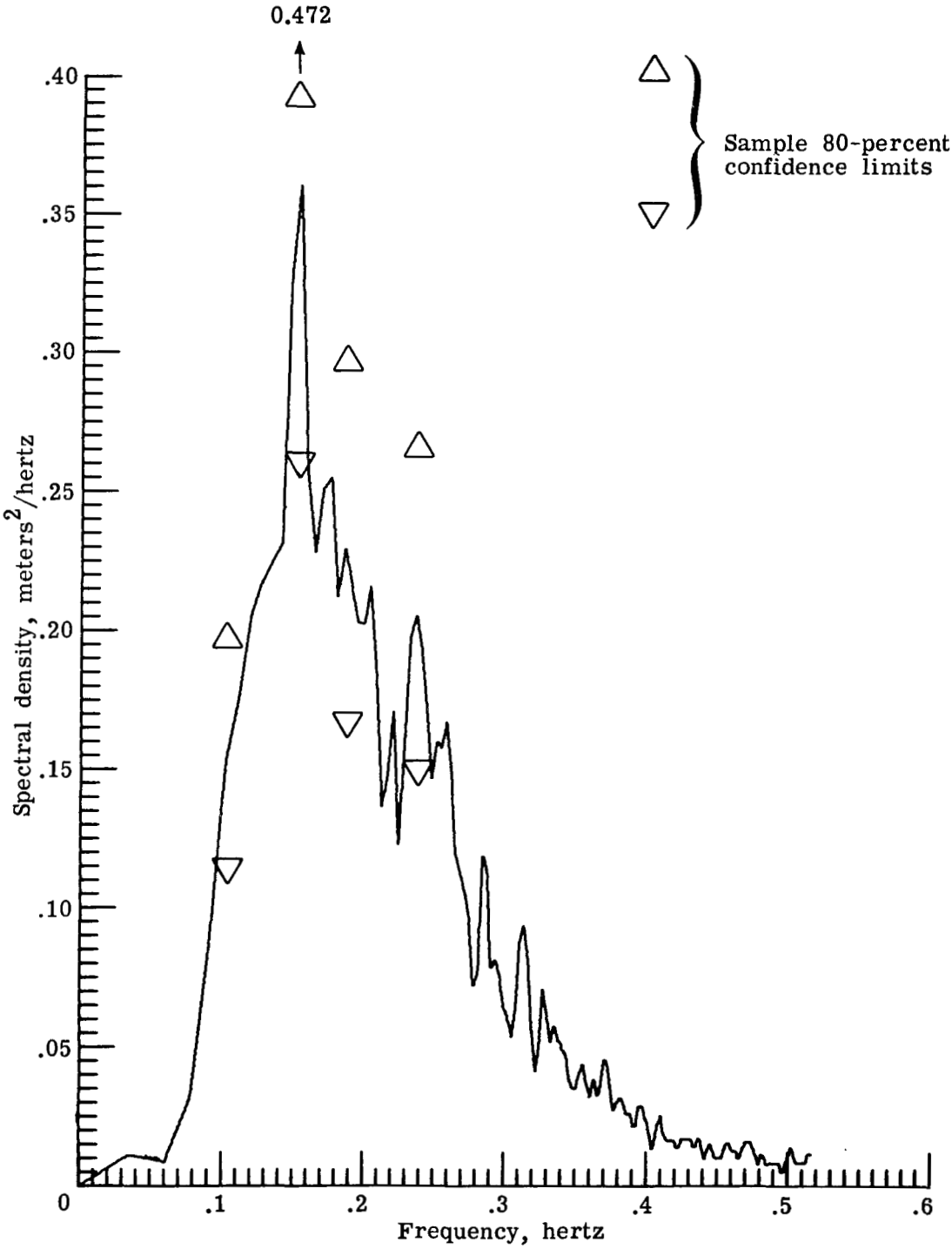

(b) Segment 4; $\bar{d}$ = 57 meters.

Figure 6.- Continued.

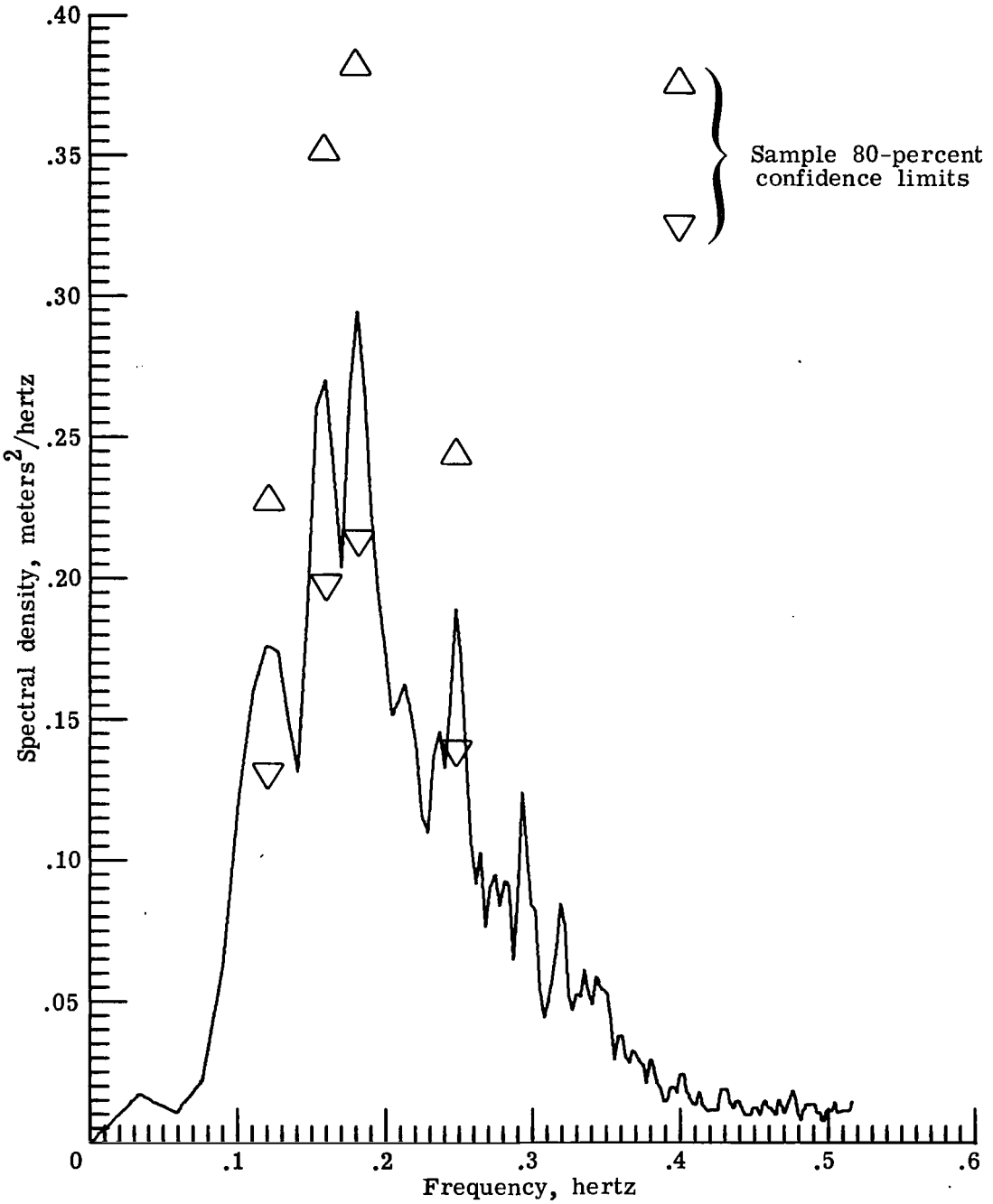

(c) Segment 5; $\bar{d}$ = 51 meters.

Figure 6.- Continued.

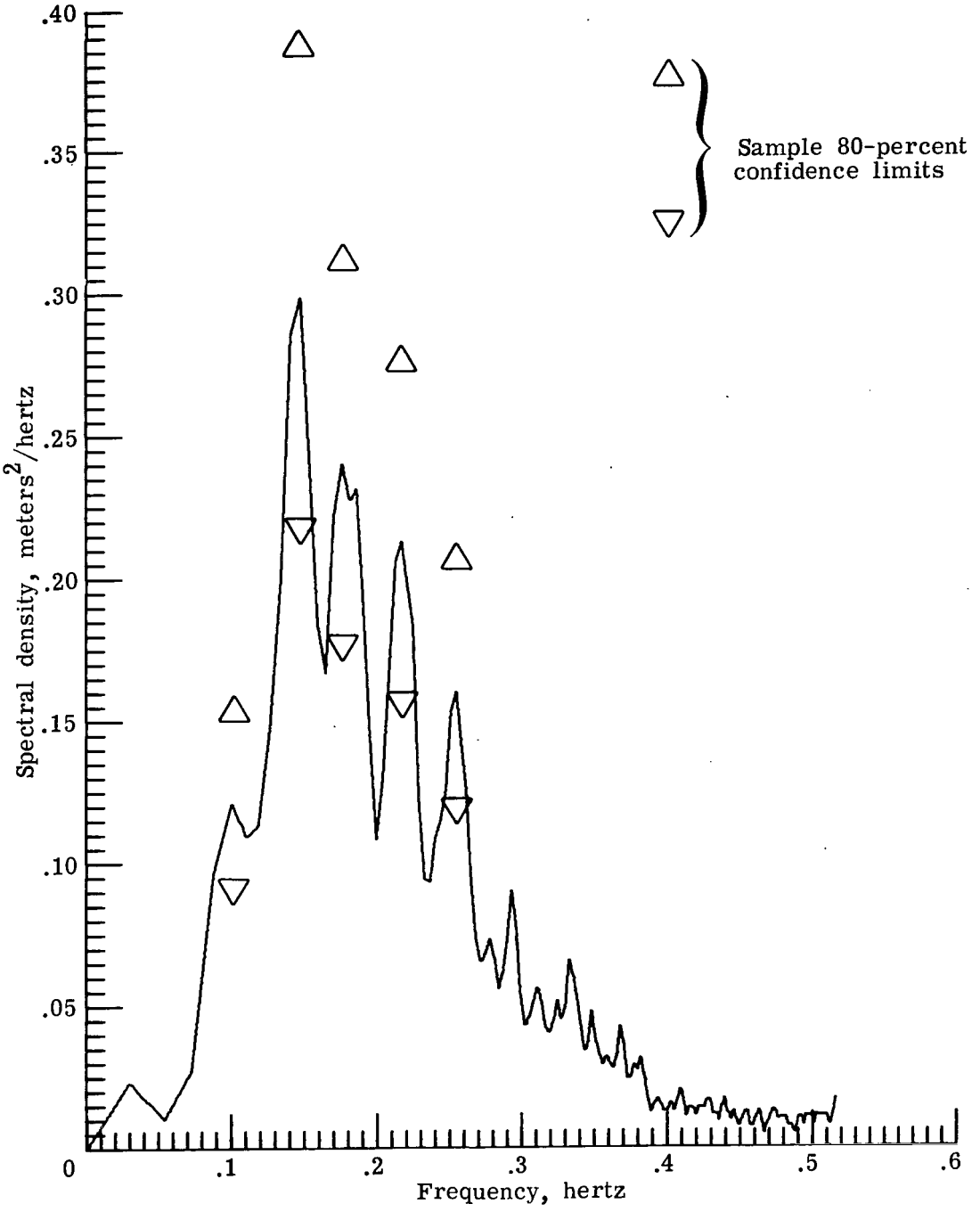

(d) Segment 6; $\bar{d}$ = 43 meters.

Figure 6.- Continued.

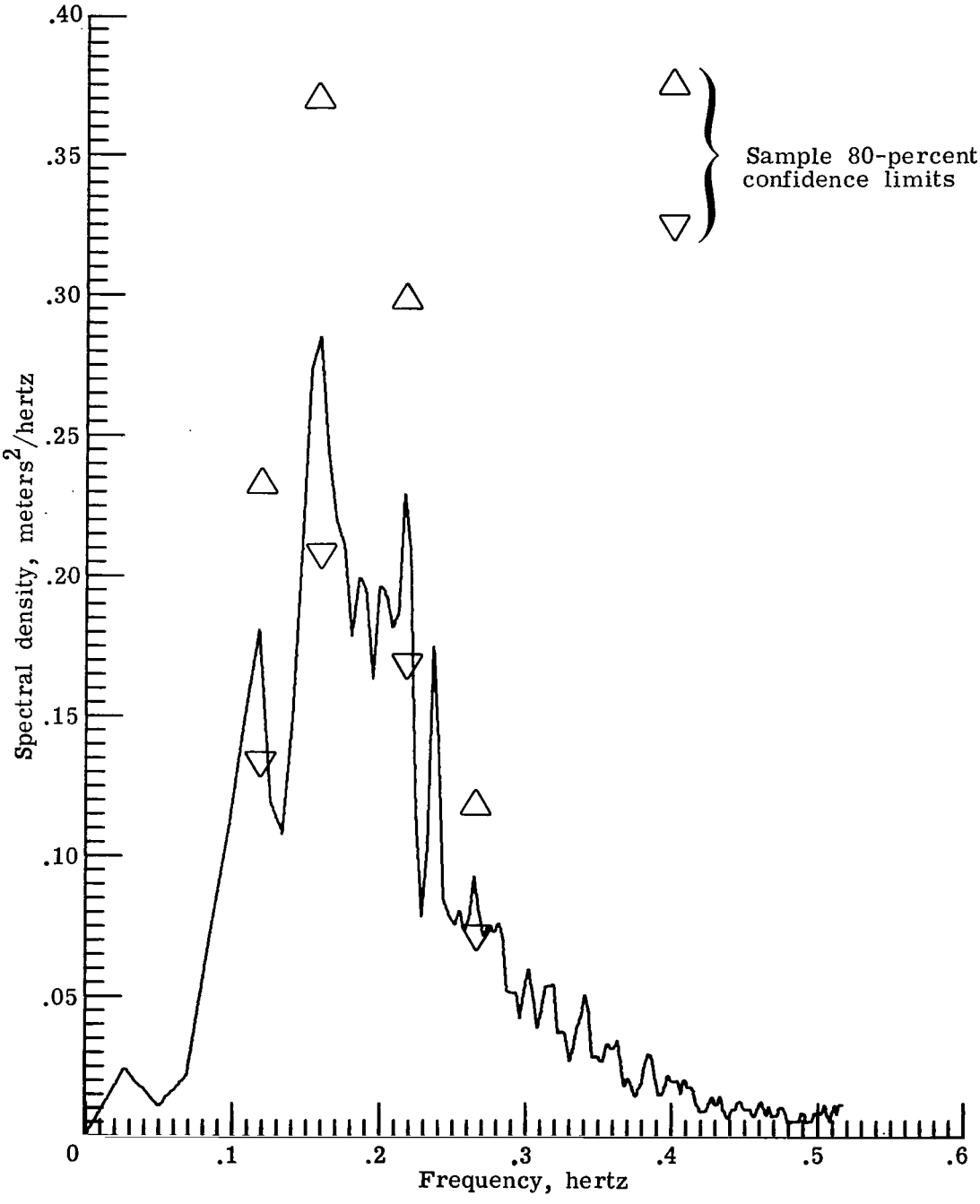

(e) Segment 7; $\bar{d}$ = 36 meters.

Figure 6.- Continued.

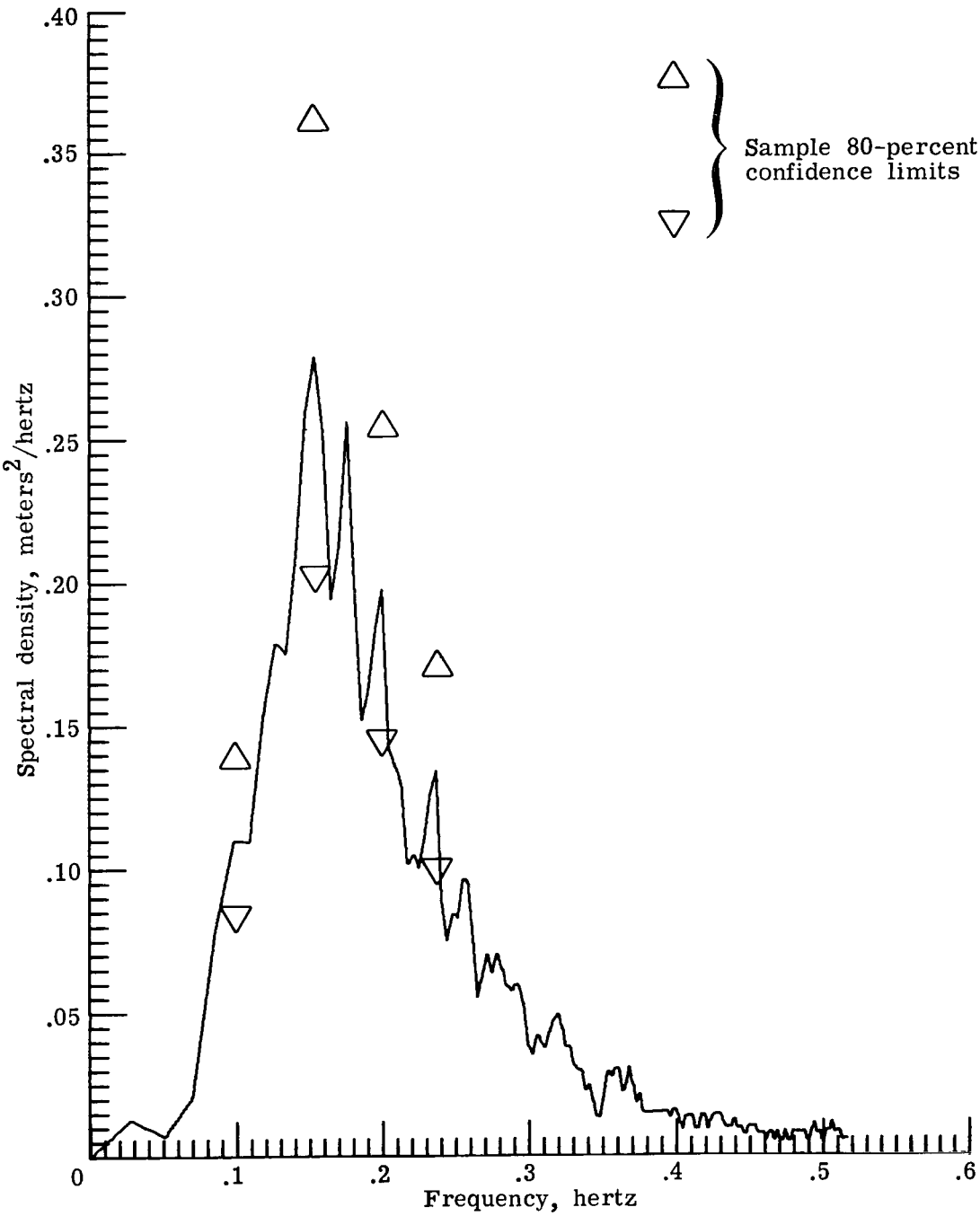

(f) Segment 8; $\bar{d}$ = 38 meters.

Figure 6.- Continued.

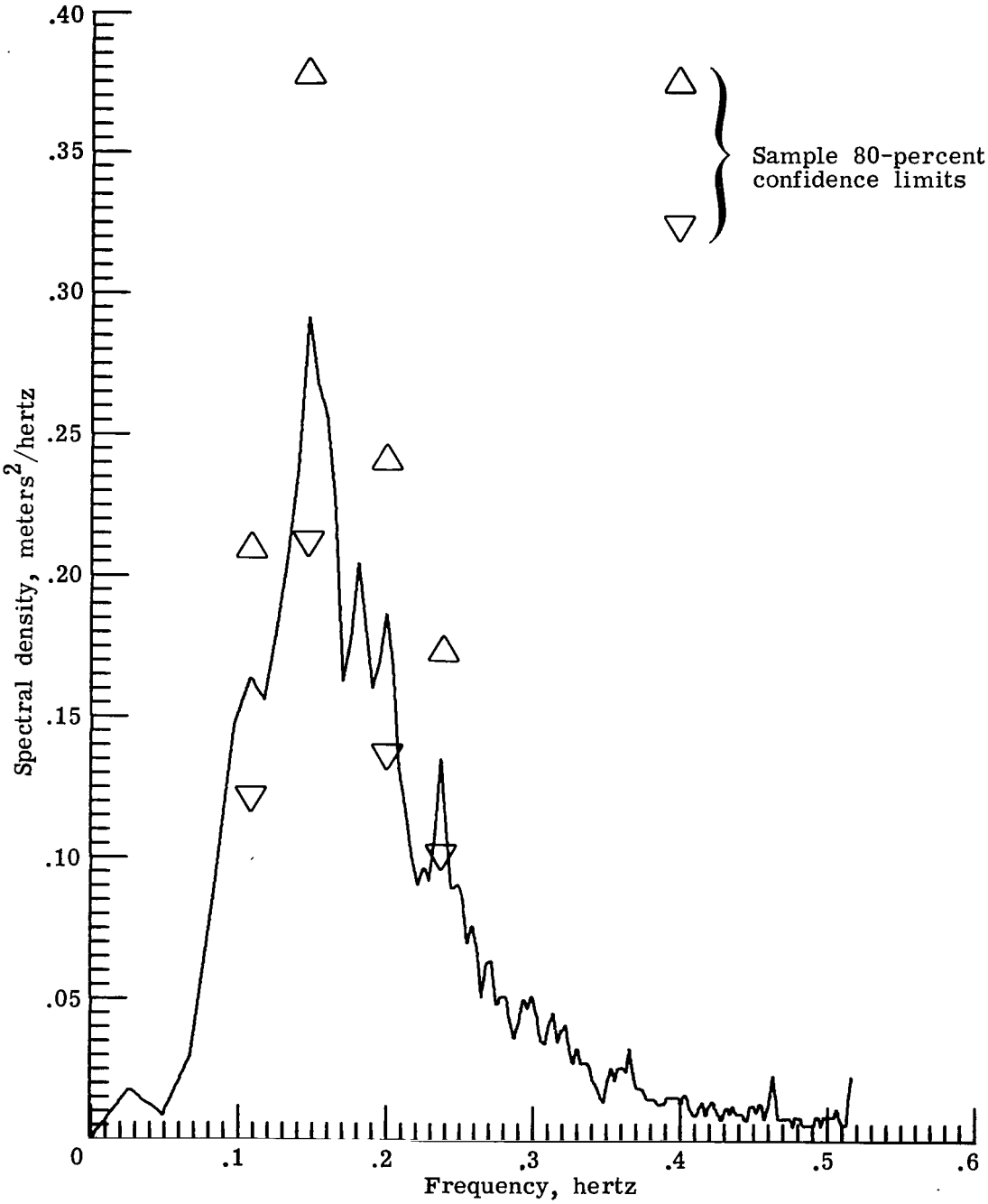

(g) Segment 9; $\bar{d}$ = 35 meters.

Figure 6.- Continued.

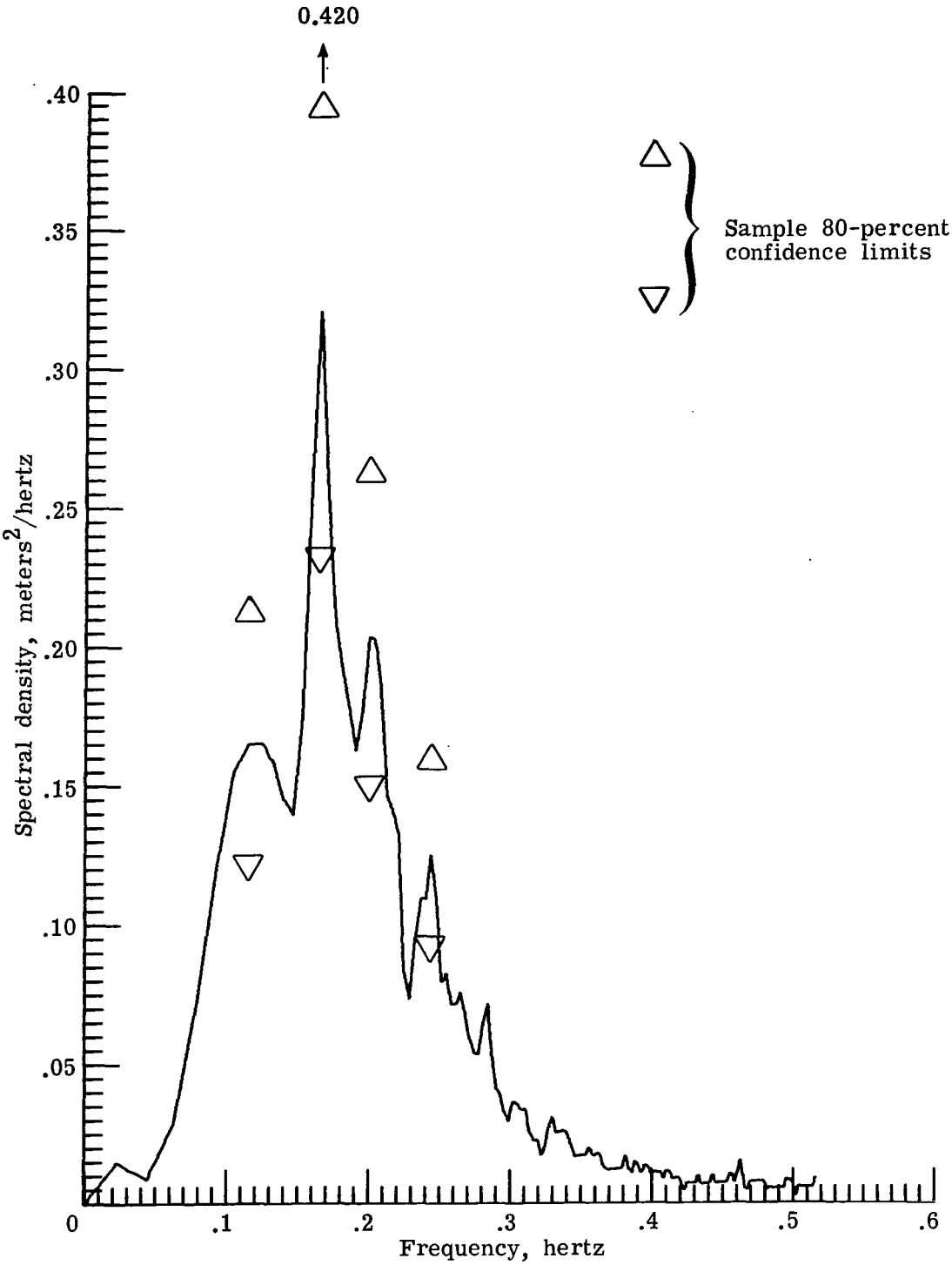

(h) Segment 10; $\bar{d}$ = 28 meters.

Figure 6.- Concluded.

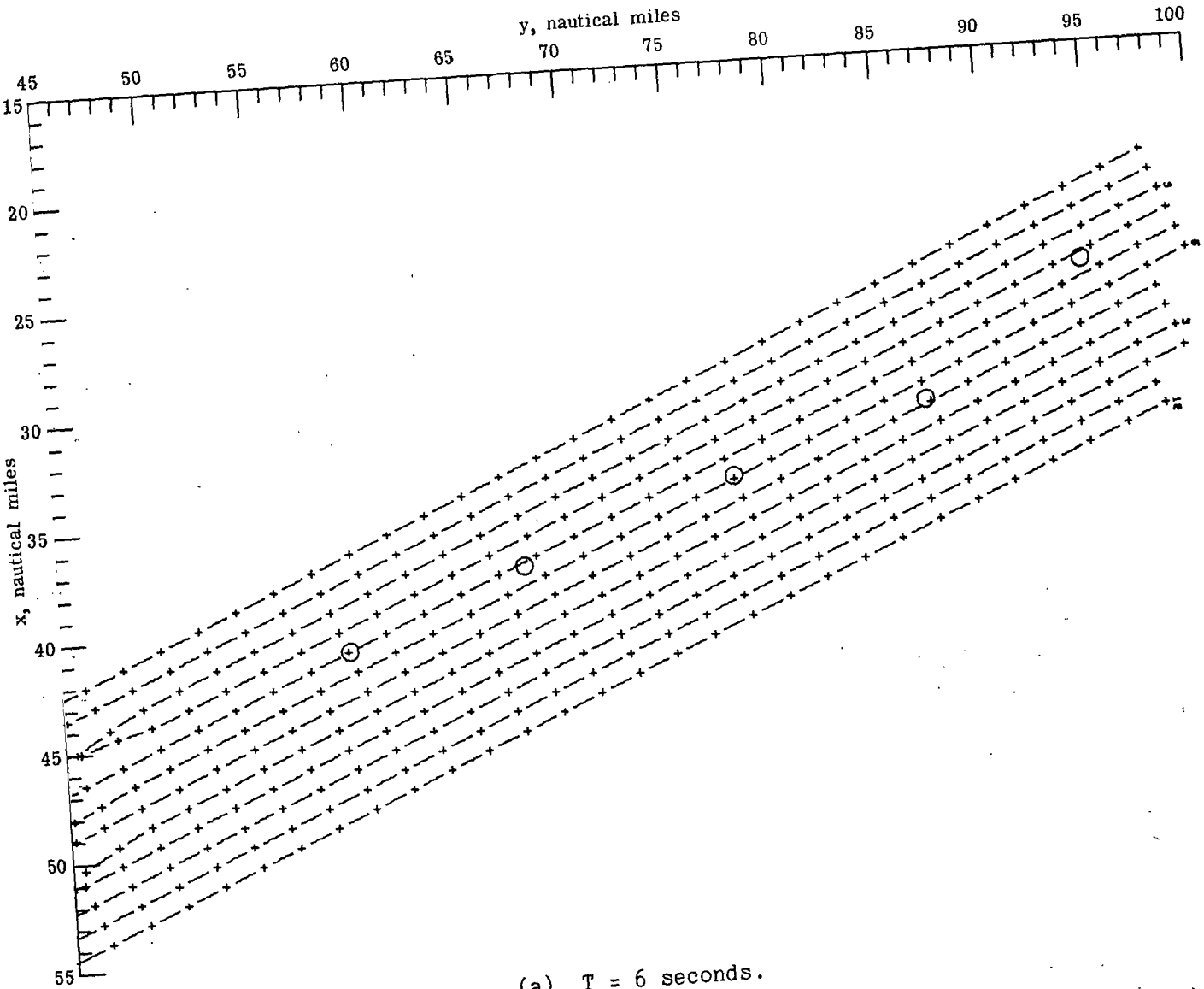

(a) T = 6 seconds.

Figure 7.- Computed refraction diagrams. $\alpha_o = 67^o$. Circular symbols denote LORAN data.

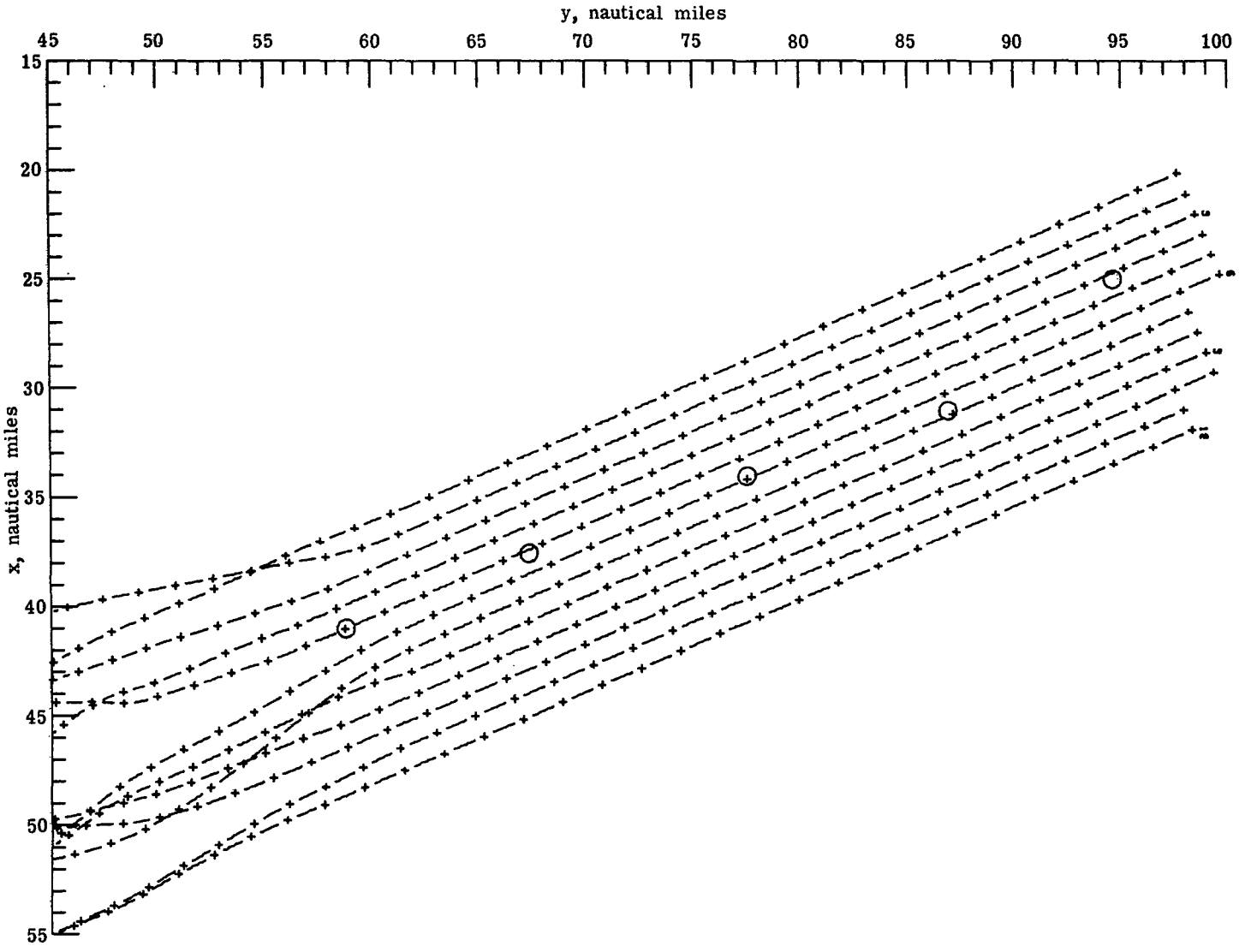

(b) T = 8 seconds.

Figure 7.- Continued.

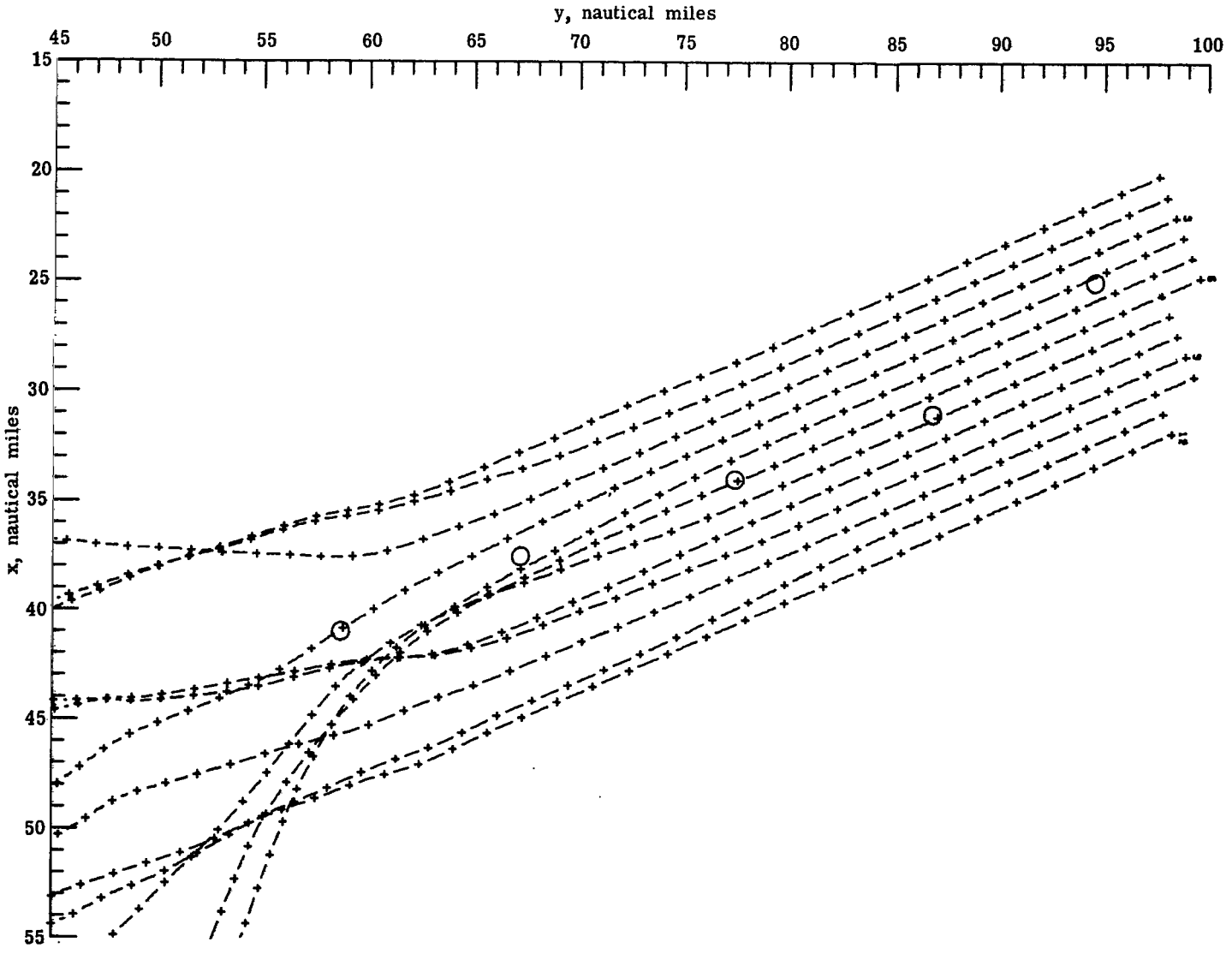

(c) T = 10 seconds.

Figure 7.- Continued.

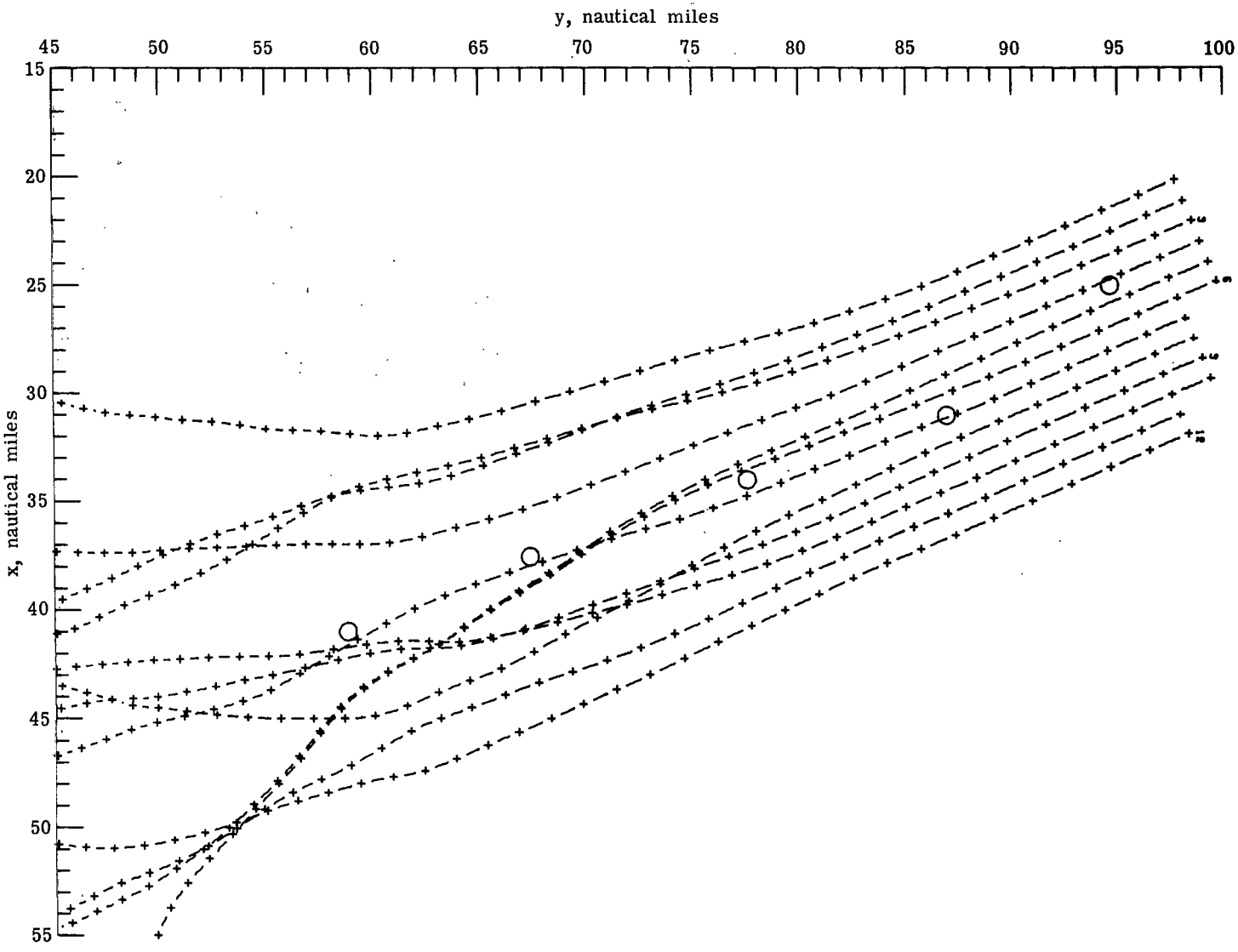

(d) T = 12 seconds.

Figure 7.- Continued.

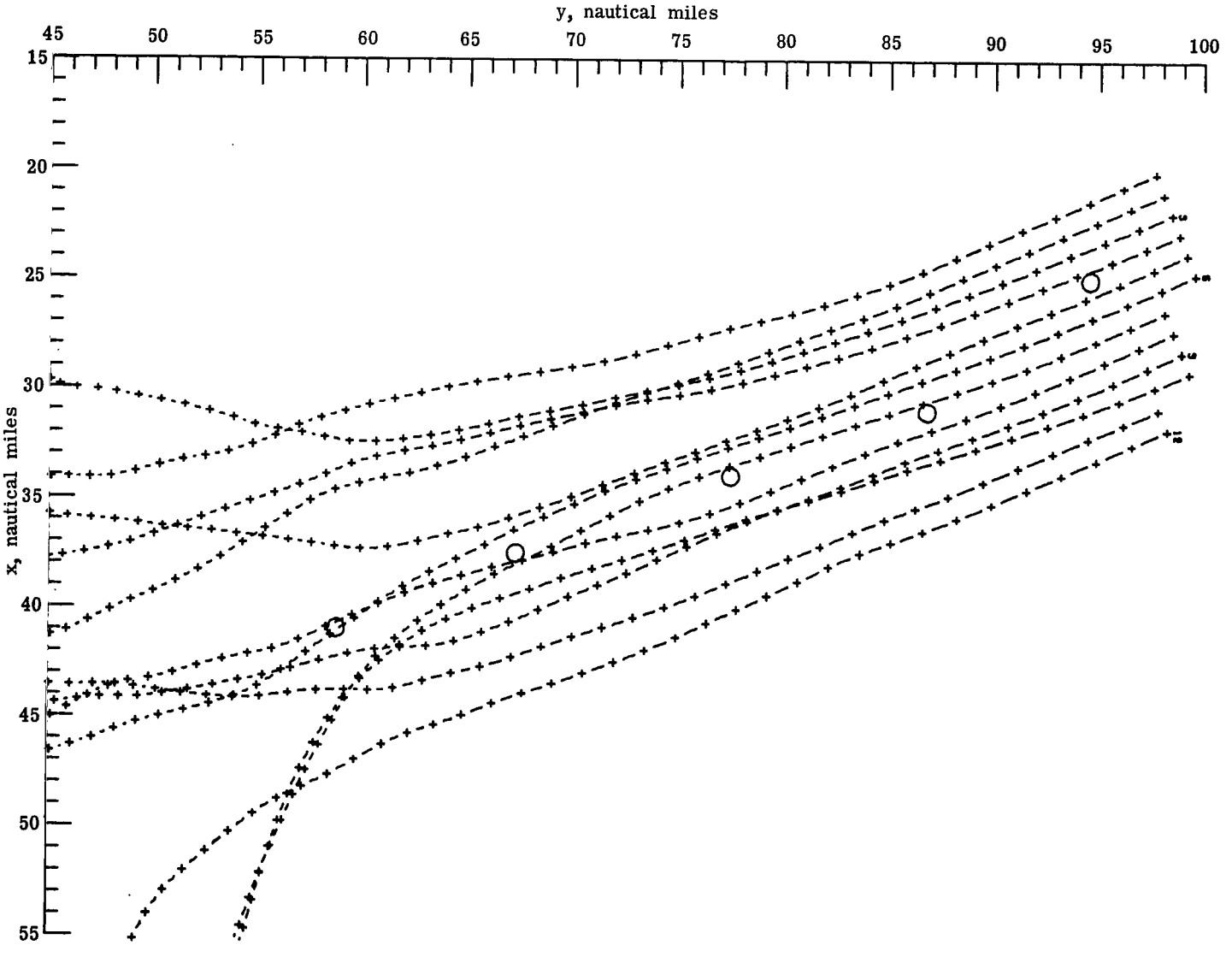

(e) T = 14 seconds.

Figure 7.- Concluded.

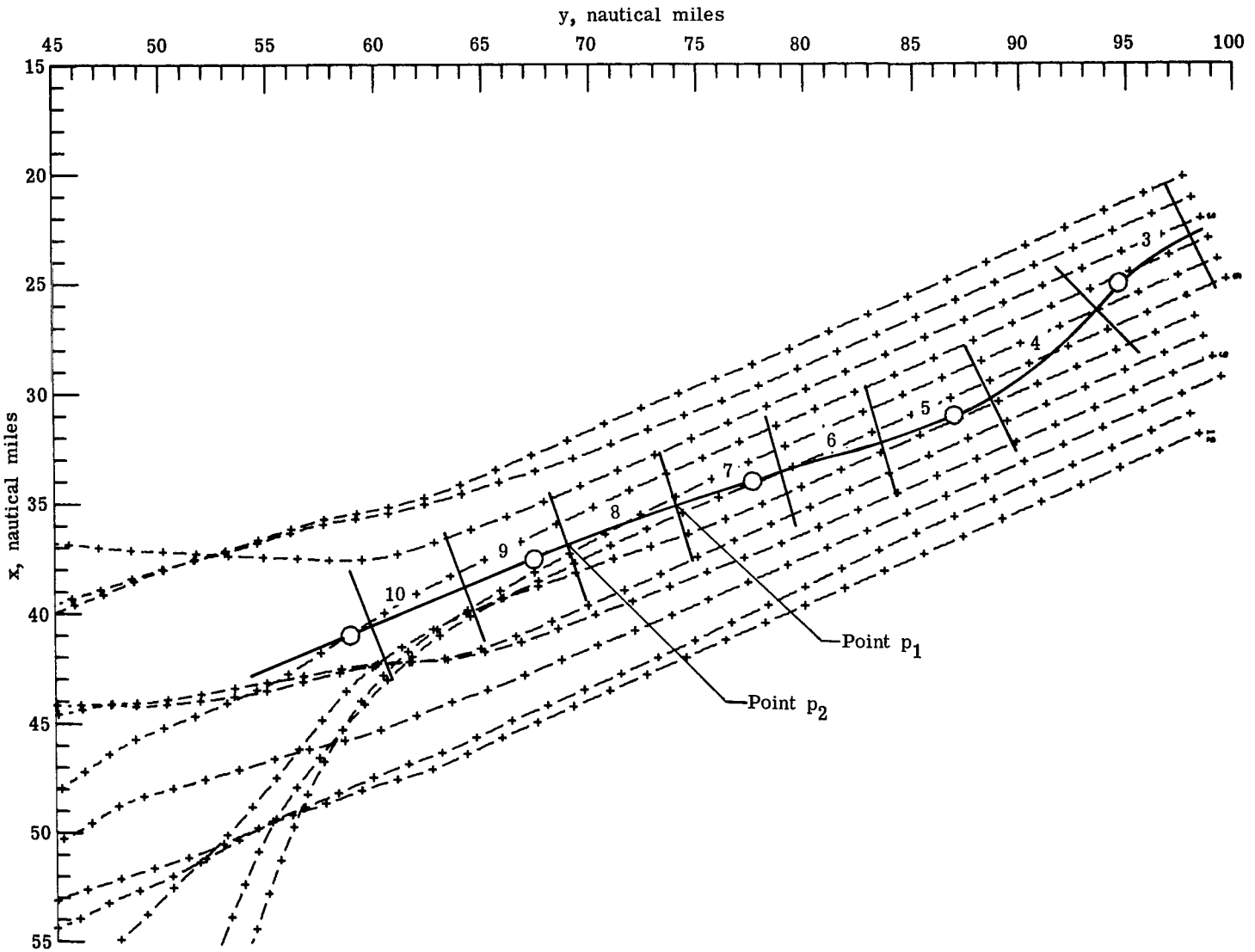

Figure 8.- Computed refraction diagram for T = 10 seconds with numbered aircraft flight-track segments superimposed. Circular symbols denote LORAN data.

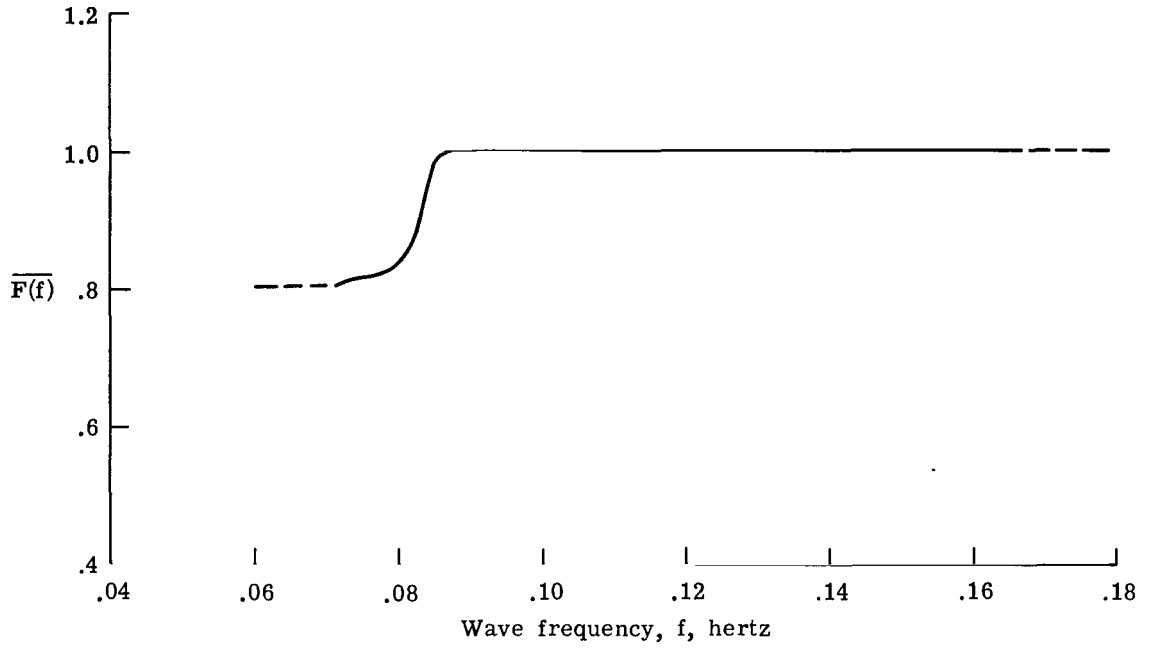

(a) Segment 3.

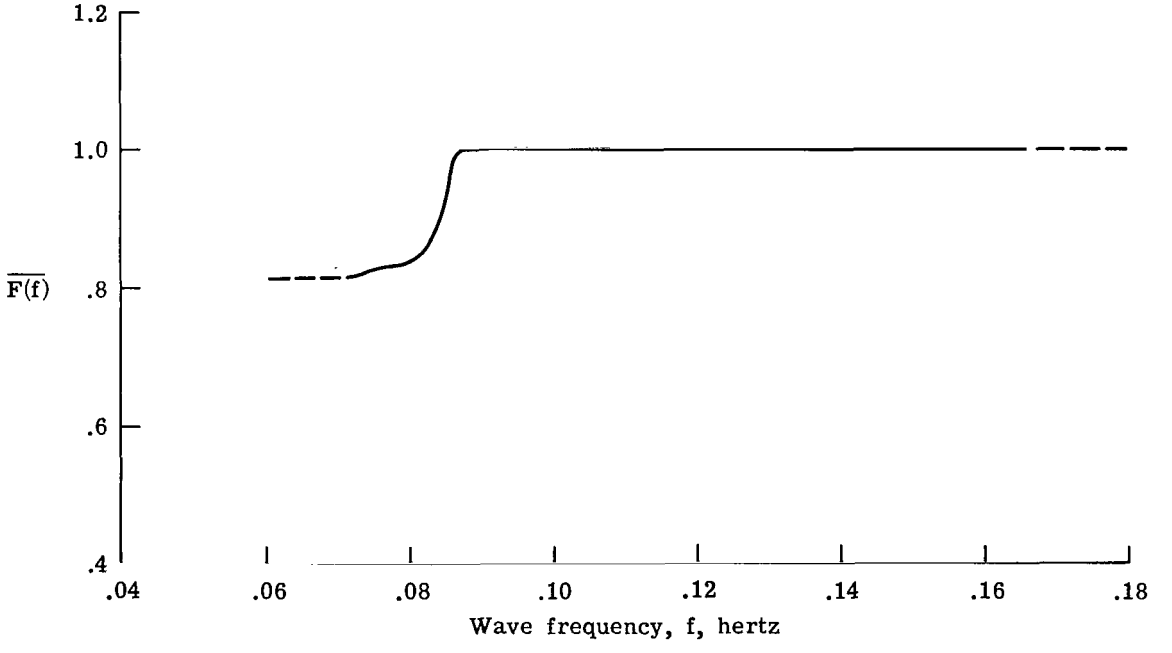

(b) Segment 4.

Figure 9.- Spatially averaged energy amplification functions for flight-track segments. Dashed curve indicates assumed values.

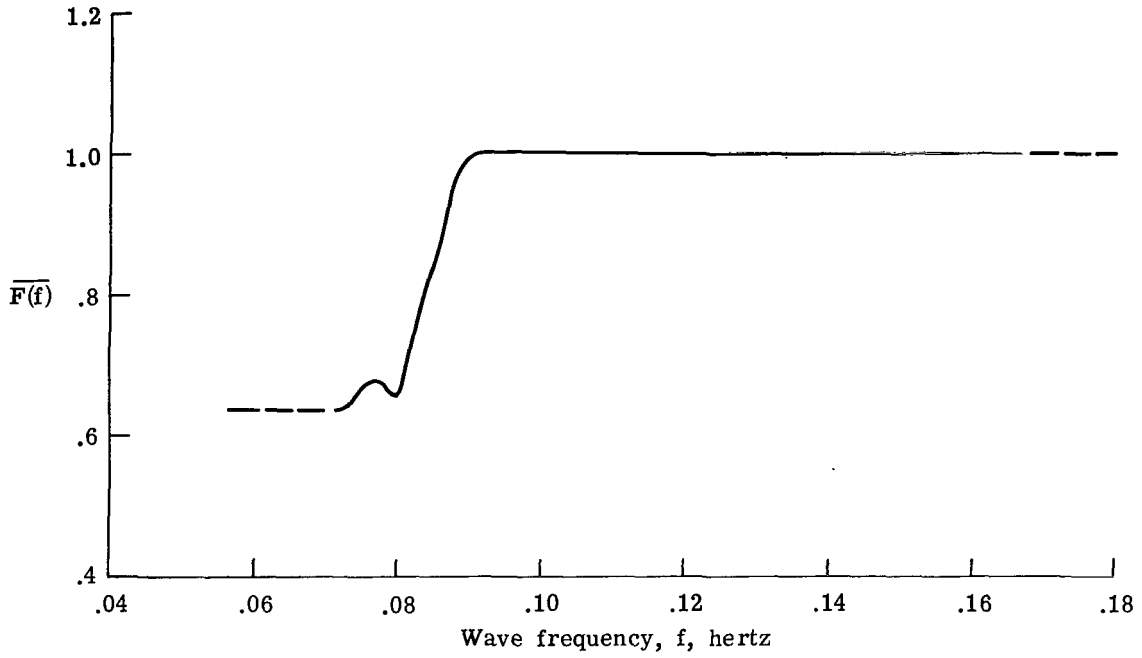

(c) Segment 5.

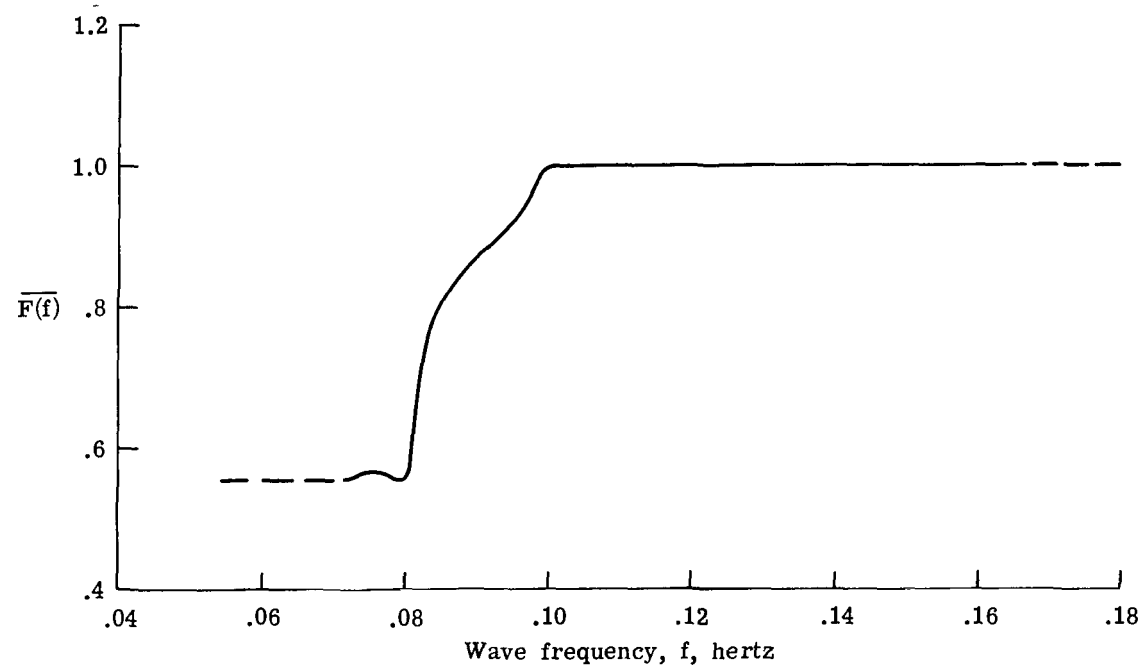

(d) Segment 6.

Figure 9.- Continued.

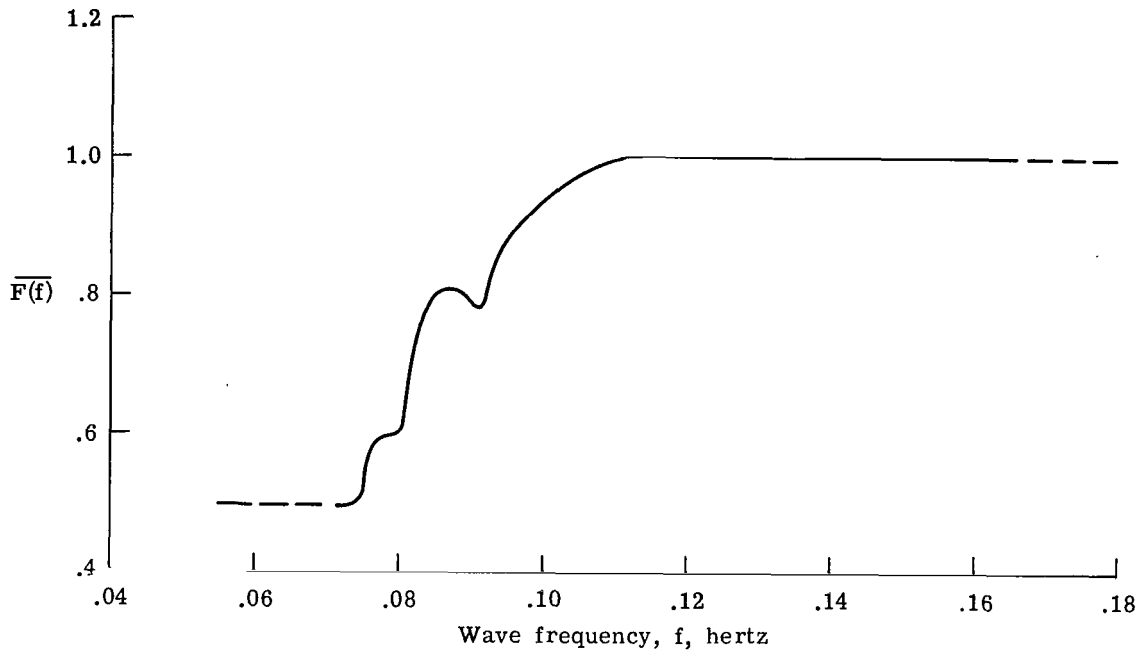

(e) Segment 7.

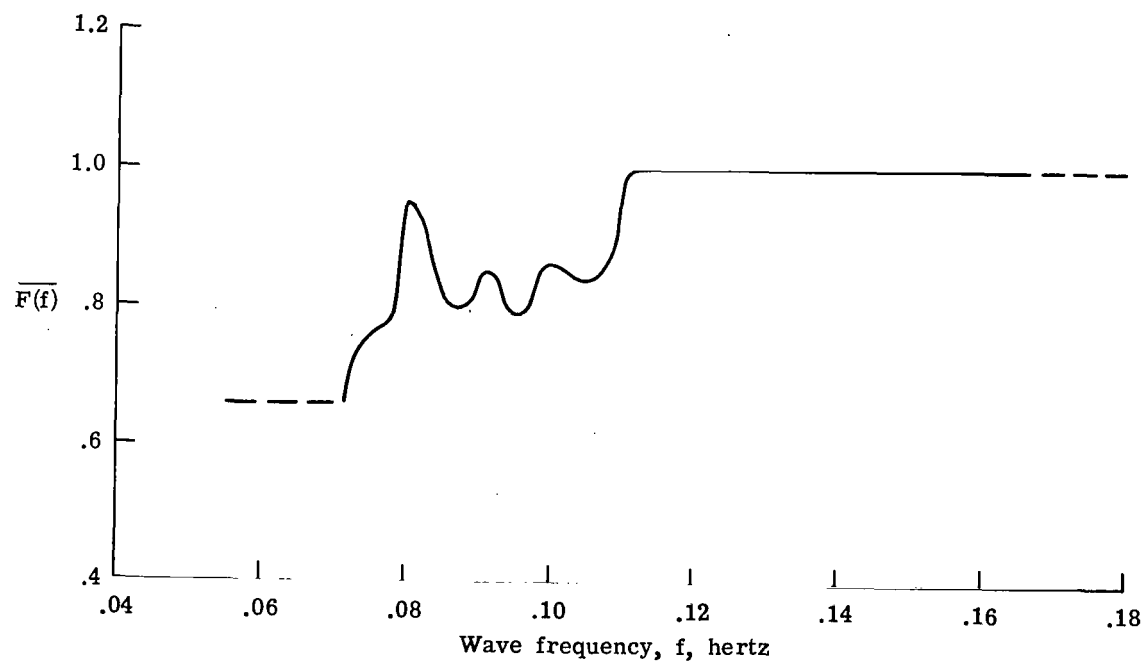

(f) Segment 8.

Figure 9.- Continued.

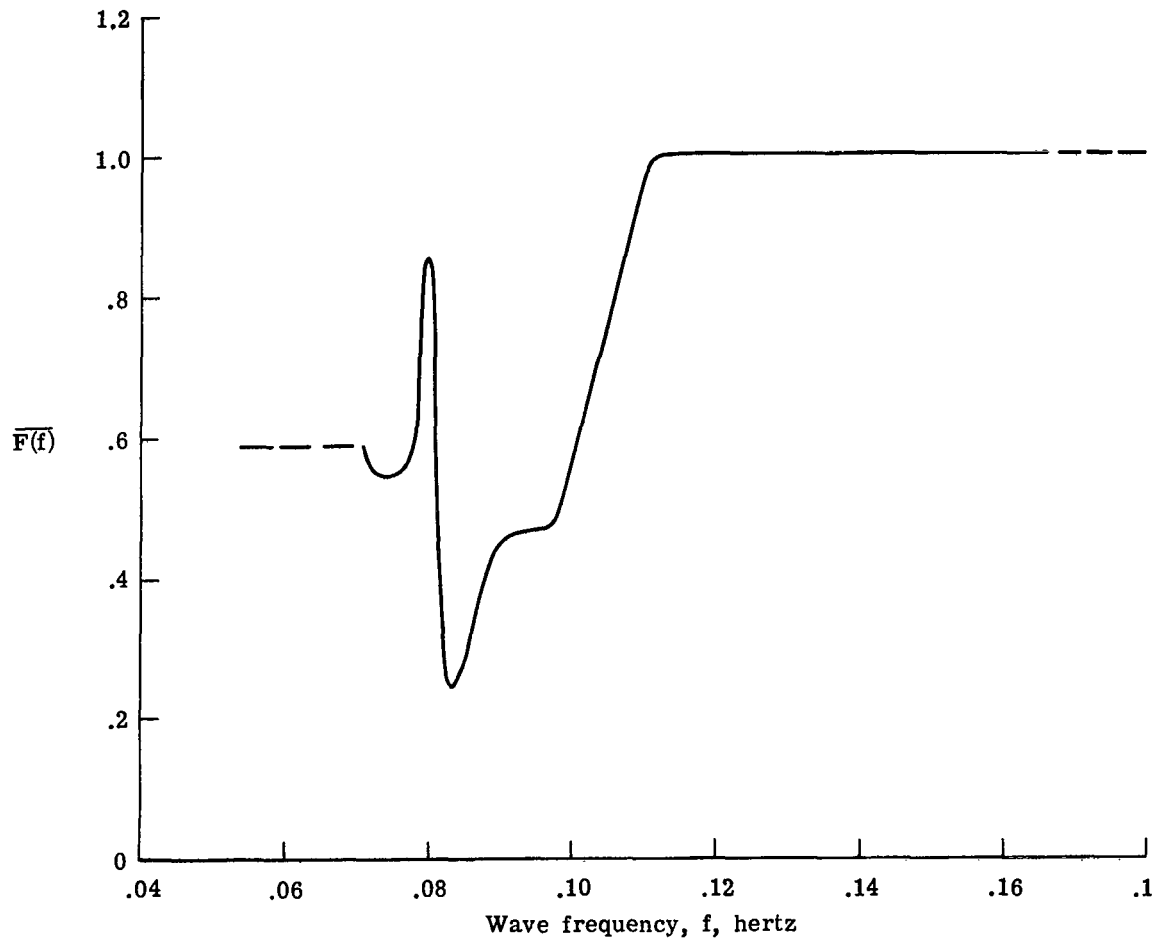

(g) Segment 9.

Figure 9.- Continued.

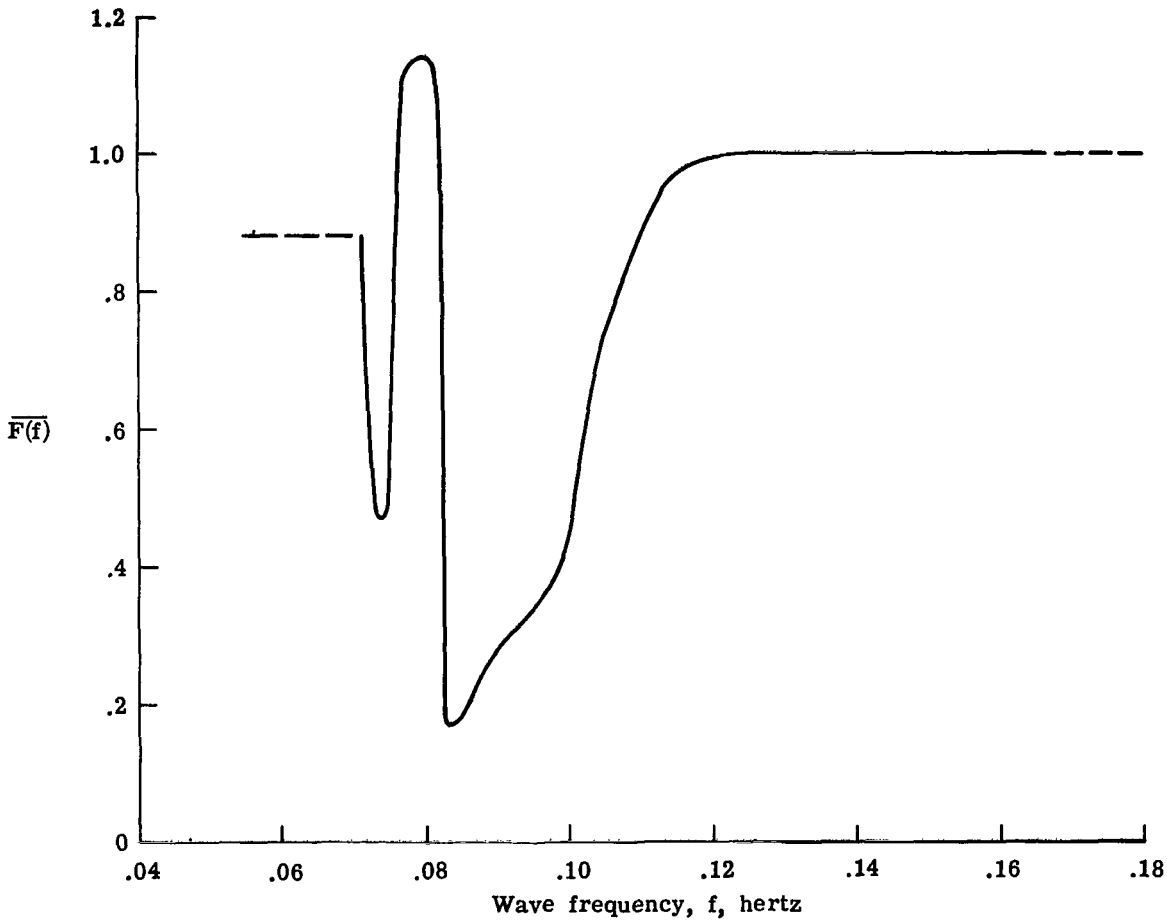

(h) Segment 10.

Figure 9.- Concluded.

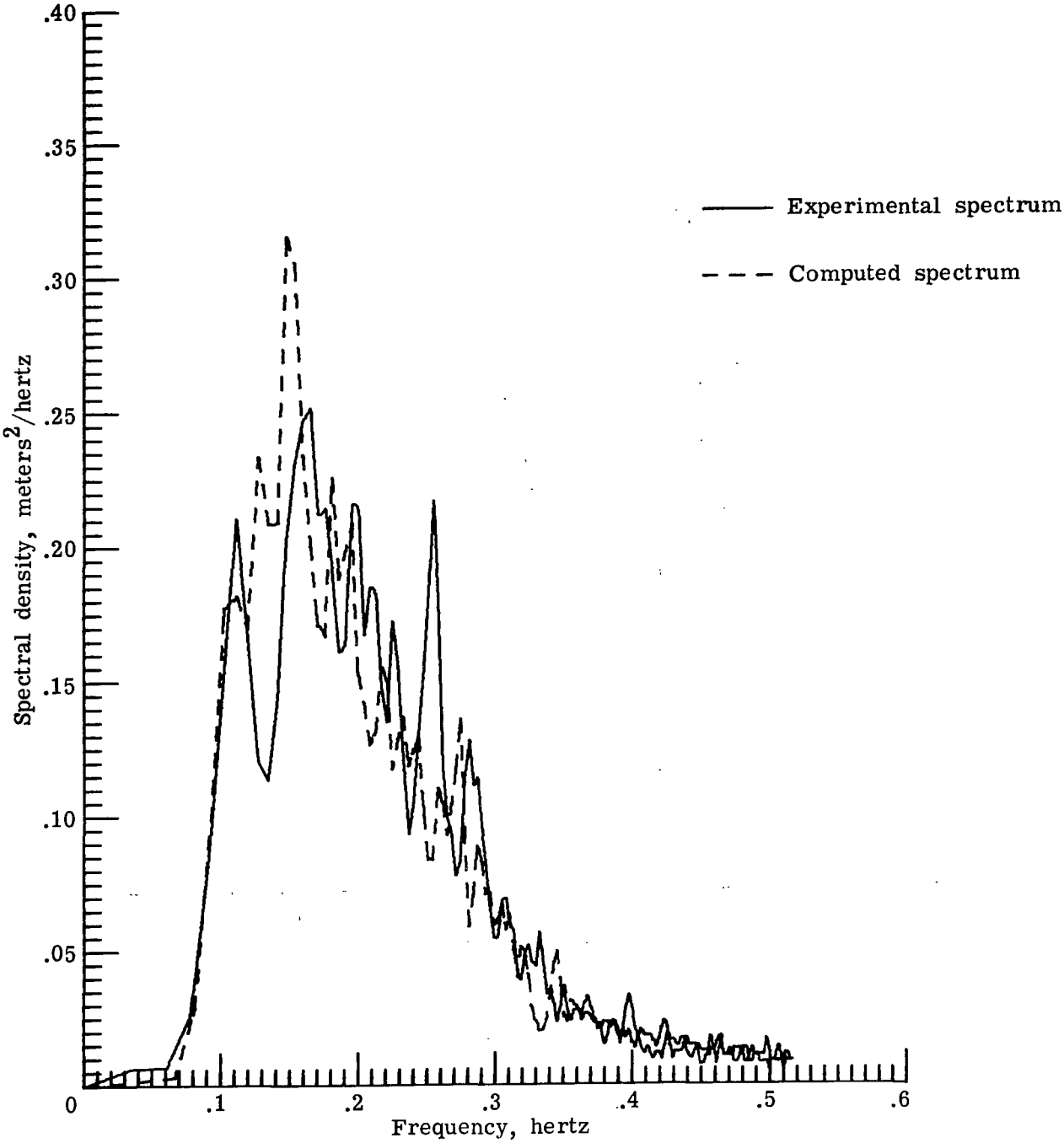

(a) Segment 3.

Figure 10.- Experimental and computed spectra for flight-track segments.

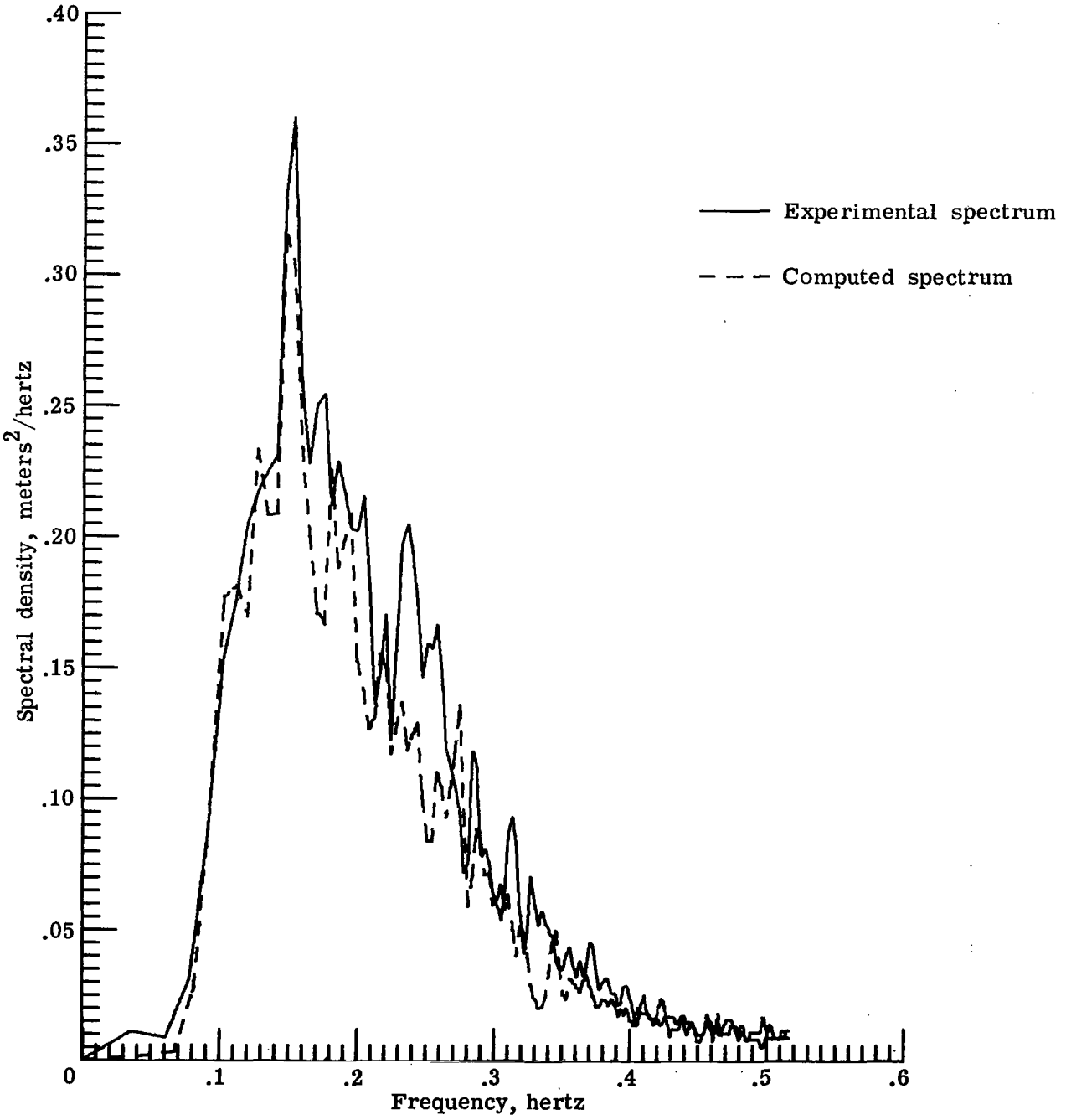

(b) Segment 4.

Figure 10.- Continued.

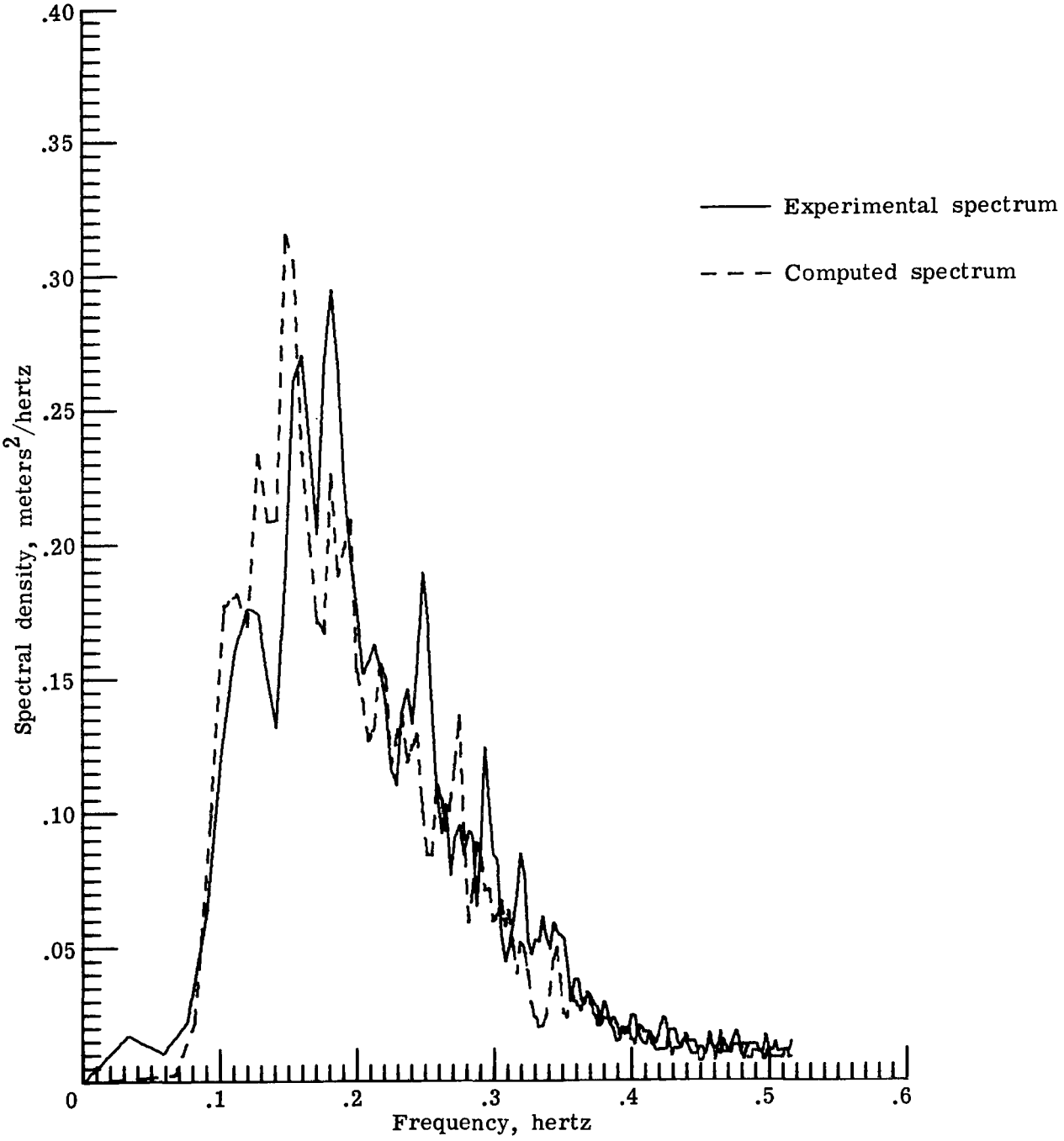

(c) Segment 5.

Figure 10.- Continued.

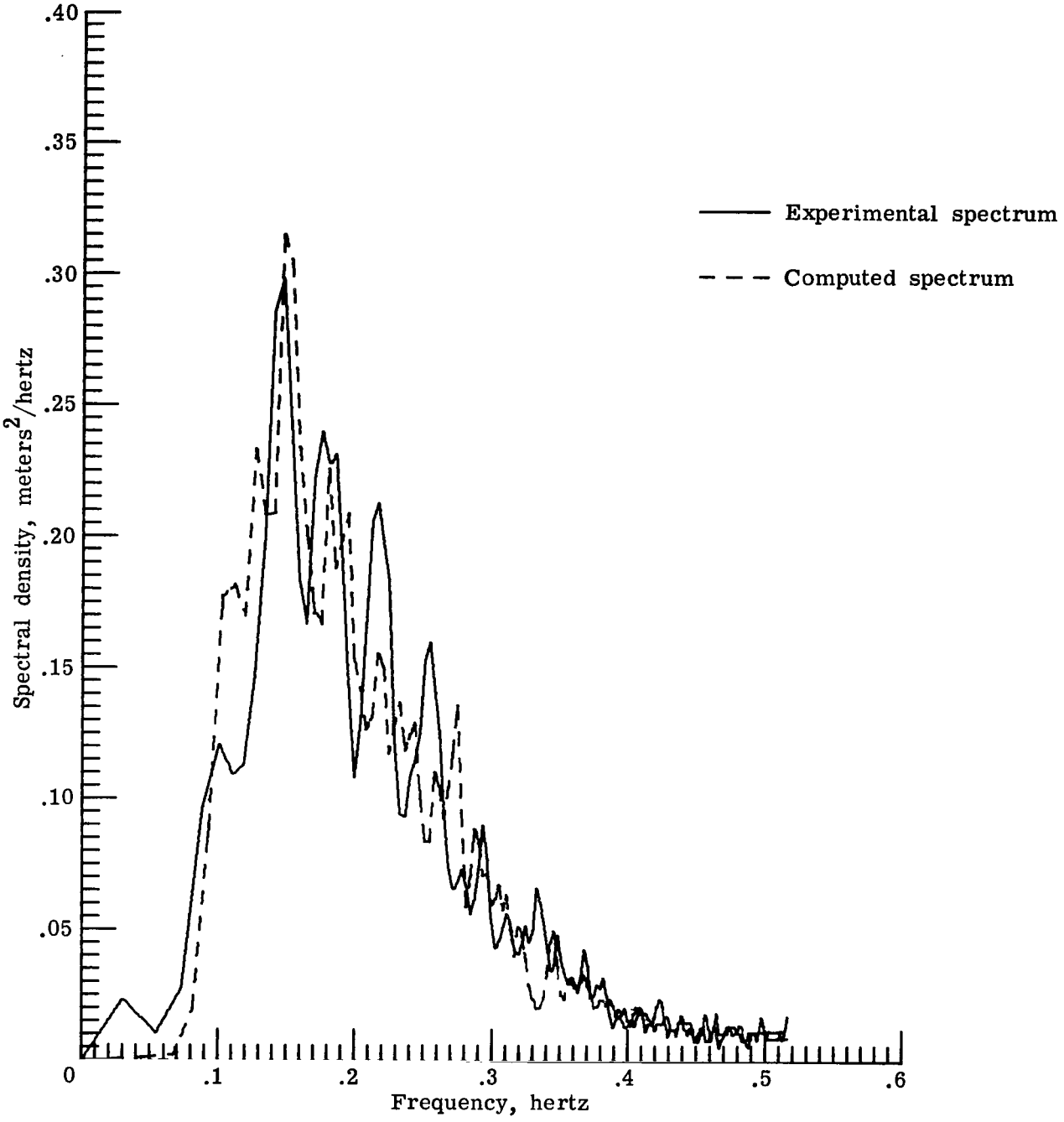

(d) Segment 6.

Figure 10.- Continued.

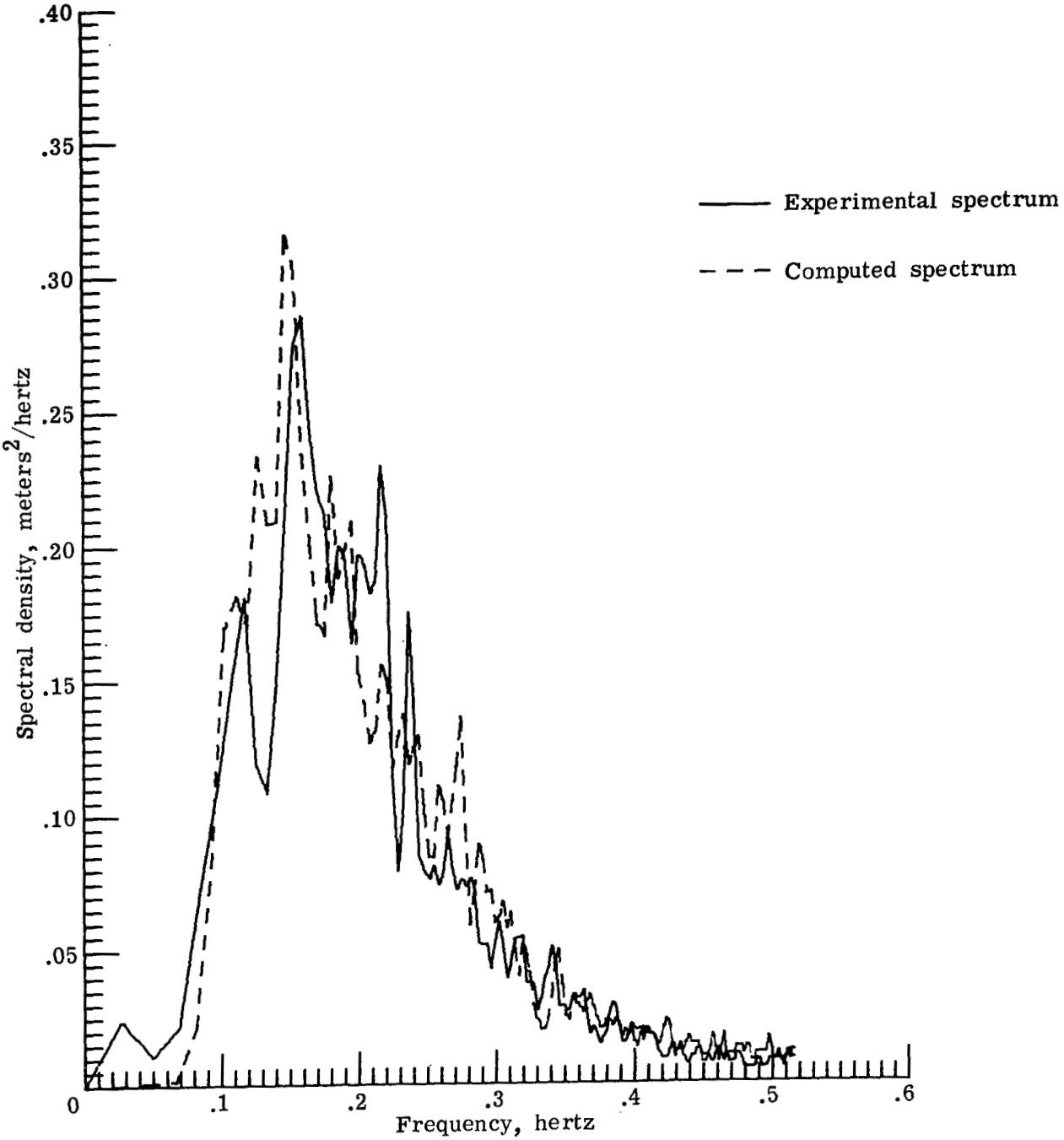

(e) Segment 7.

Figure 10.- Continued.

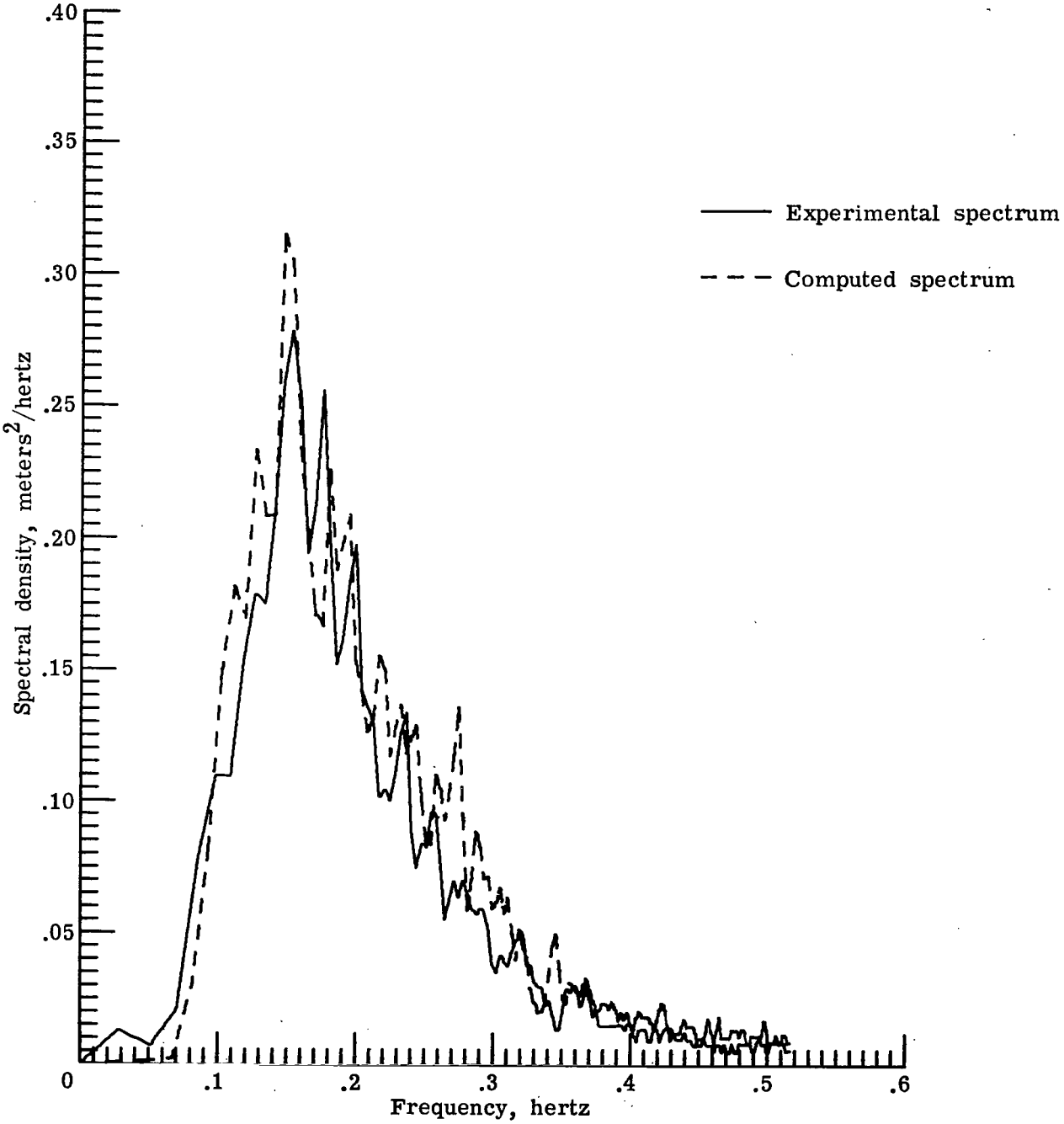

(f) Segment 8.

Figure 10.- Continued.

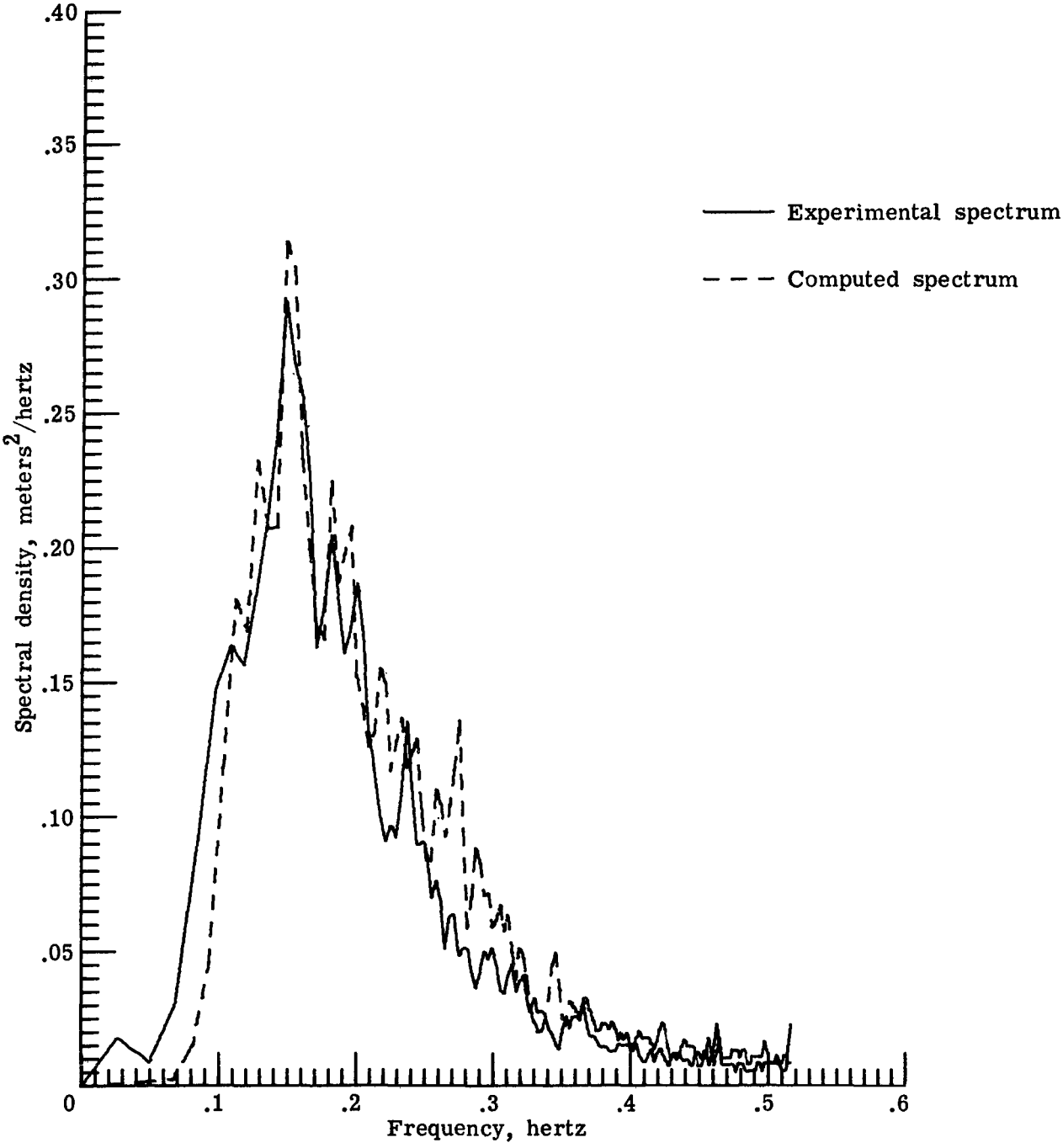

(g) Segment 9.

Figure 10.- Continued.

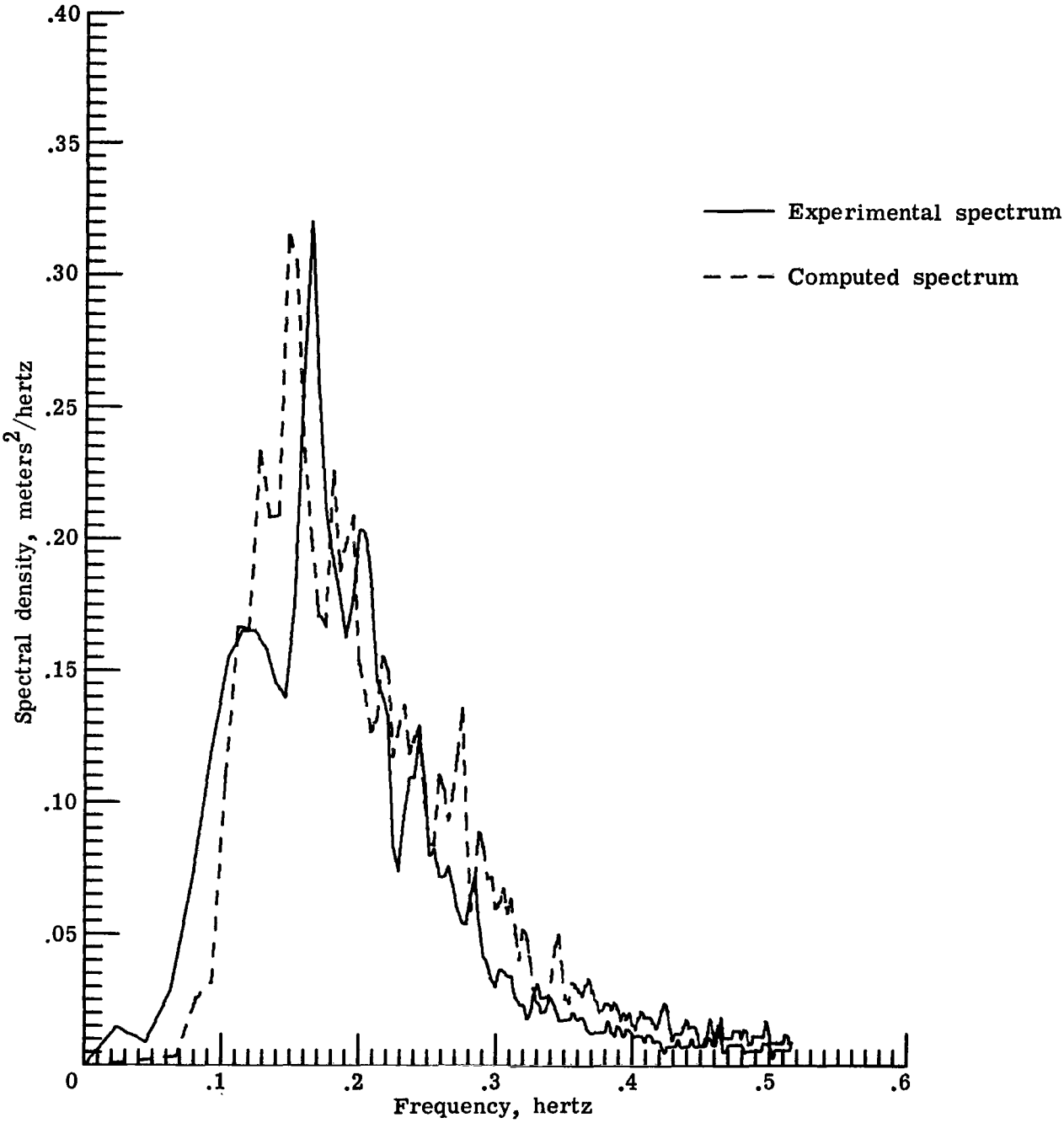

(h) Segment 10.

Figure 10.- Concluded.

"The aeronautical and space activities of the United States shall be conducted so as to contribute . . . to the expansion of human knowledge of phenomena in the atmosphere and space. The Administration shall provide for the widest practicable and appropriate dissemination of information concerning its activities and the results thereof."

—NATIONAL AERONAUTICS AND SPACE ACT OF 1958

NASA SCIENTIFIC AND TECHNICAL PUBLICATIONS

TECHNICAL REPORTS: Scientific and technical information considered important, complete, and a lasting contribution to existing knowledge.

TECHNICAL NOTES: Information less broad in scope but nevertheless of importance as a contribution to existing knowledge.

TECHNICAL MEMORANDUMS: Information receiving limited distribution because of preliminary data, security classification, or other reasons. Also includes conference proceedings with either limited or unlimited distribution.

CONTRACTOR REPORTS: Scientific and technical information generated under a NASA contract or grant and considered an important contribution to existing knowledge.

TECHNICAL TRANSLATIONS: Information published in a foreign language considered to merit NASA distribution in English.

SPECIAL PUBLICATIONS: Information derived from or of value to NASA activities. Publications include final reports of major projects, monographs, data compilations, handbooks, sourcebooks, and special bibliographies.

TECHNOLOGY UTILIZATION PUBLICATIONS: Information on technology used by NASA that may be of particular interest in commercial and other non-aerospace applications. Publications include Tech Briefs, Technology Utilization Reports and Technology Surveys.

Details on the availability of these publications may be obtained from:

SCIENTIFIC AND TECHNICAL INFORMATION OFFICE

NATIONAL AERONAUTICS AND SPACE ADMINISTRATION

Washington, D.C. 20546